Industrial Crops & Products 221 (2024) 119390

Contents lists available at ScienceDirect

Industrial Crops & Products

journal homepage: www.elsevier.com/locate/indcrop

Time-series transcriptome analysis in *Primulina eburnea* reveals a key expression network in responding to high calcium stress

Endian Yang [a,b], Yi Zhang [a,b], Qin Liu [a,b], Ziyi Lei [a,b], Jie Zhang [b], Chen Feng [b,*], Hongwen Huang [a,b,*]

[a] College of Life Science, Nanchang University, Nanchang, China
[b] Jiangxi Provincial Key Laboratory of ex situ Plant Conservation and Utilization, Lushan Botanical Garden, Chinese Academy of Sciences, Jiujiang 332900, China

ARTICLE INFO

Keywords:
Calcium stress
Primulina eburnea
Time-ordered transcriptome
CNGC
TF and non-TF network

ABSTRACT

Widespread in karst areas worldwide, this extremely calcium-rich landscape is characterized by a monoculture of vegetation types and low land-capacity efficiency. The regulatory and adaptive molecular mechanisms of plant response to high calcium soils remain poorly understood. In this study, we aimed to investigate how *Primulina eburnea*, a karst-adapted species, responds physiologically and histologically to high calcium stress, and to construct a time-ordered transcriptional profile to unravel the underlying molecular mechanisms. Key findings of our study include the involvement of transcription factor families such as MYB, WRKY, and ERF in downstream regulation of biological processes activated by calcium signaling. We observed sensitivity of photosynthesis-related genes to high calcium stress, resulting in down-regulation of expression. Additionally, calcium ion transporter proteins responded early to stress, while the reactive oxygen species elimination system continued throughout. Notably, our study identifies the central role of CNGC2 in plant resistance to high calcium environments, along with the identification of the transcription factor ATML1 regulating its expression. This study provided a preliminary systematic elucidation of plant response mechanisms to high calcium stress and uncovered the potential regulatory relationships of TFs involved in this process. The findings provide a theoretical basis for crop improvement and environmental restoration in karst regions.

1. Introduction

Karst ecosystems are an important part of terrestrial ecosystems. These landscapes cover approximately 15 % of the global land area and are characterized by shallow topsoil and high levels of free calcium ions, posing challenges for plant survival (Liu et al., 2004). The unique soil conditions in this area support a valuable but delicate biodiversity, which stores an important and endangered gene pool. China has the largest area of karst distribution in the world, and rocky desertification has resulted in significant economic losses (Guo et al., 2013; Liu et al., 2023). In combating desertification, bioremediation is considered an effective strategy. However, the success of bioremediation efforts hinges on the selection of appropriate plant species capable of restoring species diversity and managing ecological issues related to rocky desertification. The most important trait for bioremediation plants in karst region is their ability to adapt to high-calcium habitats.

Calcium (Ca^{2+}) is an essential mineral that regulates plant growth and development, as well as an important component of plant cell wall structure, and can maintain the stability of cell membranes (McAinsh and Pittman, 2009; White and Broadley, 2003). Additionally, Ca^{2+} functions as signaling molecules in plant cells in response to environmental changes and modulating responses to biotic and abiotic stresses (Tian et al., 2020). Besides, calcium is a major contributor to enzymatic reactions in plants, while calcium signaling interacts with antioxidant enzyme systems and reactive oxygen species (ROS) (Bowler and Fluhr, 2000). However, it is important to maintain a low cytoplasmic concentration of calcium ions, as elevated levels can disrupt normal physiological functions within plant cells. The uptake of Ca^{2+} by plant cells is directly influenced by concentration of calcium in the soil solution. Therefore, in calcium-rich soils like those in karst regions, excessive uptakes can occur, surpassing the amount needed for proper cellular function (White and Broadley, 2003). Previous studies have demonstrated that high concentrations of calcium can inhibit plant growth by affecting photosynthesis and reducing plant growth characteristics (Wu

* Correspondence to: No. 9, Zhiqing Rd, Jiujiang, Jiangxi 332900, China.
E-mail addresses: yanged@lsbg.cn (E. Yang), zhangyi@lsbg.cn (Y. Zhang), liuqin232022@163.com (Q. Liu), leiziyi111@outlook.com (Z. Lei), louisvant@hotmail.com (J. Zhang), fengc@lsbg.cn (C. Feng), huanghw@scbg.ac.cn (H. Huang).

https://doi.org/10.1016/j.indcrop.2024.119390
Received 19 March 2024; Received in revised form 11 July 2024; Accepted 5 August 2024
Available online 9 August 2024

et al., 2014). At the cellular level, excessive calcium can interfere with calcium-dependent signaling systems, disrupt phosphate-based energy metabolism and ultimately lead to cell death (Wu et al., 2011). Therefore, maintaining intracellular calcium balance is crucial for normal plant growth, particularly in environments with high calcium concentrations, where plants must possess physiological mechanisms to prevent excessive uptake of calcium ions (Borer et al., 2012).

Research has predominantly focused on calcium ions as signaling molecules, while little attention has been paid to plant responses to calcium stress, despite some progress in Arabidopsis (Cheng et al., 2005; Wang et al., 2017b). Various plants have different calcium requirements, and plant cells have evolved precise regulatory mechanisms to limit cytosolic Ca^{2+} accumulation through various Ca^{2+} channels and transporter proteins (Jia et al., 2022). Ca^{2+}/H^{+} exchanger antiporters (CAXs) are widely localized in membrane-contained organelle, particularly in the tonoplast, where they transport cytosolic calcium ions into the vacuole. In *Arabidopsis*, the *cax3* mutant lines showed hypersensitivity to high Ca^{2+} stress, whereas the *cax1/cax3* double mutant showed even higher Ca^{2+} stress sensitivity compared to the single mutants (Cheng et al., 2005). Moreover, plants have the ability to adapt to high calcium stress by restricting the influx of calcium ions from outside the cytoplasm into the cytoplasm. Cyclic nucleotide-gated channel 2 (CNGC2) is involved in the absorption of calcium ion in leaf cells (Verret et al., 2010). The *cngc2* mutants exhibit sensitivity to increased exogenous calcium ion concentrations. While, the *cngc2* mutant grows normally at 0.1 mM Ca^{2+} and reduced growth compared to wild type under culture conditions of 20 mM Ca^{2+} (Wang et al., 2017b). Despite the established importance of CNGC2 in plant response to calcium stress, its upstream regulators have not been previously reported. Additionally, these limited calcium tolerance mechanisms were mostly reported in model but not karst plants, highlighting the need for further research in this area.

Gesneriaceae, a botanical family with a global distribution spanning tropical to temperate regions, encompasses many species of great commercial value, serving as herbal medicines and ornamental flowers (Dong et al., 2018; Serain et al., 2021; Verdan and Alves Stefanello, 2012). Among these, *Primulina eburnea* (Hance) Yin Z. Wang, commonly known as Yan-bai-cai, belongs to the genus *Primulina* within Gesneriaceae. It thrives in the southern and south-western regions of China, where its habitat is typical karst landscapes. *Primulina eburnea* is a valuable traditional Chinese medical herb, of which quinones, terpenoids and flavonoids are the main active ingredients (Yang et al., 2023). It mainly functions on alleviating coughs and inflammation, and also has great potential in the development of antitumor drugs (Yang et al., 2023). Cultivated for many years in Guizhou and Guangxi, China, *P. eburnea* stands out for its remarkable capacity to accumulate calcium, both total and bioactive calcium, in its leaves, making it an excellent candidate for phytogenic calcium supplementation (Qi et al., 2013). Moreover, due to its adaptation to high-calcium karst habitats, *P. eburnea* plays a significant role in vegetation restoration efforts in rocky desertification areas, thereby mitigating economic losses associated with land degradation.

In this study, to understand the mechanisms of karst plant adaptation to high calcium soils, we constructed a time-ordered gene co-expression network (TO-GCN) under calcium stress in *P. eburnea*. Combined with weighted correlation network analysis (WGCNA) and transcription factors (TFs) regulatory sub-networks, we identified the core gene *PebCNGC2* in response to high calcium stress and its upstream transcription factor PebATML1. This is the first comprehensive mapping of plant transcriptional profiles in response to high calcium stress at the time sequence level. The hierarchical regulatory relationship between TFs and non-TFs is described, and preliminary elucidation of the molecular mechanism of plant adaptability to the high soil calcium environment, which provides a theoretical basis for the breeding of calcium stress-tolerant crops and important economic crops, as well as an important guide to the restoration of vegetation in karst areas and the management of desertification.

2. Materials and methods

2.1. Plant materials and calcium treatment

Primulina eburnea seedlings were transplanted into individual pots (12 cm diameter) one week after seed germination and cultured for two months, with regular application of Hoagland's nutrient solution every 4 days to maintain normal growth. Then, the seedlings were subjected to calcium stress treatment at various concentrations including 0, 25, 50, 75, 100, and 125 mM for one month. Each seedling was treated with 150 mL of Hoagland's nutrient solution containing different concentrations of calcium chloride every four days. Each treatment included five biological replicates. The plant samples were cultivated under standardized conditions in a growth chamber, with a light intensity of 5000 lux, a photoperiod of 16 hours light/8 hours dark, a temperature of 25°C, and a humidity of 60 % to ensure consistent growth conditions. Based on phenotypic observations, a concentration of 100 mM was selected for a duration of 20 days using a $CaCl_2$ solution. At specific time points (0, 6, 12, 24, 48 hour (h), and 5, 10, 20 day (d)), roots and second pair of leaves from each seedling were collected. Samples collected at each time point were divided into two portions. One portion was rapidly frozen in liquid nitrogen used for enzyme activity assays, while the other portion was used for transcriptome sequencing. Sampling was repeated three times.

2.2. Analysis of antioxidant enzyme activities and histological observation

After treatment with 100 mM calcium solution at different time points, the contents of proline (Pro), catalase (CAT), superoxide dismutase (SOD), and peroxidase (POD) activities were determined using respective detection kits (Solarbio, Beijing, China) following the manufacturer's protocol. The root vitality of roots in root samples was determined with the TTC-method detection kit (BC5270, Solarbio). Relative electrical conductivity was measured as described previously (Zhao et al., 2023). For histological observation, leaves were fixed in glutaraldehyde, dehydrated in a gradient of ethanol solution, and then infiltrated and embedded in paraffin followed by sectioning with the rotary microtome (Yang et al., 2021).

2.3. RNA extraction and transcriptome analysis

Total RNA of all samples was extracted using EASYspin Universal Plant RNA Kit (Aidlab, Beijing, China). Sequencing libraries were constructed by BioMarker Co., Ltd. (Beijing, China), and cDNA library was sequenced on the Illmina NovaSeq 6000 paired-end sequencing platform with a read length of 150 bp. Raw reads were filtered by removing adapters and low-quality reads with the criterion described by our previous study (Feng et al., 2017). Clean reads were mapped to the *P. eburnea* reference genome (Yi et al., 2022) using HISAT2 v2.1.0 (Kim et al., 2015). StringTie (version 2.1.3) (Pertea et al., 2015) was used to quantify gene expression from reads to the transcripts per million (TPM) values. Differentially expressed genes (DEGs) in pairwise comparisons were identified using DEseq2 v1.24.0 (Love et al., 2014) with criteria of $|\log2\ (\text{fold change})| \geq 1$, *padj*-value < 0.01. GO enrichment and KEGG pathway analyses for DEGs were performed using the OmicShare tools, a free online platform for data analysis (https://www.omicshare.com/tools). All transcripts, excluding genes with low expression levels (TPM < 10), were used to generate co-expression modules through WGCNA analysis package in R (Zhang and Horvath, 2005).

2.4. Time-ordered gene co-expression network

The TO-GCN is an effective method for identifying moderators of the

time series response process and their regulatory networks, revealing hierarchical regulatory relationships of TFs (Chang et al., 2019). A TF gene (*Peb08082*), showing a peak expression at the start and down-regulation thereafter, was selected as a seed gene. DEGs were categorized into TFs and non-TFs, and the Pearson correlation coefficient (PCC) values between each pair of TF and non-TF genes were calculated. Then, the TO-GCN was generated, containing TFs and non-TFs with a threshold PCC > 0.9, to illustrate the co-expression relationships. The regulatory networks were visualized using Cytoscape (Xu et al., 2021).

2.5. Quantitative real-time PCR analysis

Total RNA extracted from all samples used for RNA-seq was also used for qRT-PCR. The first-strand cDNA was synthesized using the HiScript II Q RT SuperMix for qPCR kit following the instructions (R223–01, Vazyme). All primer pairs for selected genes were listed in Table S1. The experiment was performed according to the described protocol (Zhang et al., 2024) using the Bio-Rad CFX96 real-time PCR detection system (Hercules, CA, USA). The expression level of the candidate gene was calculated using the $2^{-\Delta\Delta Ct}$ method relative to the internal control gene, *PebGAPDH* (Zhang et al., 2024).

2.6. Subcellular localization

The *PebCNGC2* coding sequence was excised from the stop codon, fused to a GFP protein, and cloned into a vector carrying a CaMV35S promoter. The recombinant vectors were transiently expressed in *Nicotiana benthamiana* leaves using the Agrobacterium infection system. AtCBL1::mCherry was used as a plasma membrane marker (Batistic et al., 2010). Tobacco seedlings were cultured for three days, after which the leaves were cut for fluorescence observation under a confocal laser scanning microscope (FV3000, OLYMPUS, Japan).

2.7. Yeast one-hybrid assay

The coding sequences of *PebATML1*, *PebANL2* and *PebBZR1* were cloned into the pGADT7 vector, and the promoter of *PebCNGC2* was cloned into the pAbAi vector. These constructs were transformed into the Y1HGold yeast strain and tested for interaction in the SD base/-Leu-Ura medium with Aureobasidin A. The empty pGADT7 vector was used as negative control, and the p53-AbAi reporter vector served as a positive control.

2.8. Dual-Luciferase assay

The coding sequence of *PebATML1* was cloned into the pGreenII 62-SK vector, and the promoter of *PebCNGC2* was cloned into the pGreenII 0800-LUC vector. These recombinant vectors were delivered into *N. benthamiana* leaves using the Agrobacterium infection system for transient expression. After three days, the injected leaves were photographed using the Tanon 6600 imaging system (Tanon, Shanghai, China) and the fluorescence intensities was quantified using Image J software (Schneider et al., 2012).

2.9. Analysis of calcium tolerance in transgenic Arabidopsis thaliana

The CDS sequence of *PebCNGC2* was cloned into a vector containing the 35S promoter. Transgenic *Arabidopsis* plants were generated using Agrobacterium-mediated floral dip method. The seeds of both wild-type (Col-0) and homozygous T3 transgenic lines were sterilized with 5 % sodium hypochlorite for 5 minutes, then sown on 1/2 MS medium. After vernalization at 4°C for 2 days, the plates were transferred to a growth chamber. One week later, seedlings were transplanted into potting soil and cultured normally for three days. Subsequently, they were regularly irrigated with a 50 mM $CaCl_2$ solution, with water-treated groups serving as controls. After two weeks, the fresh weight and calcium content of the leaves were measured, and photosynthesis was assessed. Each experiment was repeated three times.

2.10. Statistical analysis

Data were statistically analyzed using SPSS software (version 26; IBM, Armonk, NY, USA). ANOVA followed by Duncan's multiple range test was performed for data computation, and the results were presented as means ± SD of a minimum of three biological replicates. Statistically significant differences ($P < 0.05$) were indicated in the graphs.

3. Results

3.1. Effect of $CaCl_2$ treatment to Primulina eburnea

To assess the impact of different concentration of calcium ion treatments on the growth of *P. eburnea*, 3-month-old plants were irrigated with solution containing 0, 25, 50, 75, 100, 125 mM $CaCl_2$, and the resulting phenotypes were observed. Overall, plant growth decreased with increasing calcium ion concentration. Although no significant phenotypic differences were observed between treatments below 50 mM (Fig. S1), growth inhibition occurred with calcium toxicity above 75 mM. Notably, after one month of treatment at 100 mM, significant necrosis appeared at the growth points of plant leaves (Fig. 1A). The necrotic areas rapidly expanded to encompass the entire leaf, ultimately leading to the death of the plants. Therefore, the lowest lethal concentration was set at 100 mM, and physiological responses were examined at eight time points: 0, 6, 12, 24, 48 h and 5, 10, 20 d. As the treatment duration extended, the leaves yellowed after ten days, followed by noticeable decay of the young leaves after twenty days (Fig. 1B). Histological examination revealed that leaf necrosis initially occurred near the leaf veins, originating from the xylem and spreading outward (Fig. 1C and D). Upon $CaCl_2$ treatment, the homeostasis of ROS was disrupted, and several key enzymes in the antioxidant system responded significantly to high calcium stress. Specifically, the content of CAT increased gradually, peaking at 12 h, and then slowly decreased but remained relatively high (Fig. 1E). The SOD content showed a slight initial increase, followed by a decrease and then resumed an upward trend after 48 h (Fig. 1F). POD content sharply increased after 10 days of treatment, reaching a level approximately four times greater than the untreated condition (Fig. 1G). Additionally, as the treatment progressed, the Pro content steadily increased, while the root vitality decreased, and the relative electrical conductivity of leaves gradually increased (Fig. 1H–J). These results provide strong evidence that lethal concentration of calcium stress could trigger a series responses of *P. eburnea*.

3.2. Transcriptomic analysis

To elucidate the underlying mechanisms of *P. eburnea* in response to high calcium stress, we conducted transcriptome analysis on leaf and root samples at multiple time points. After filtration, a total of 36 RNA-seq libraries were generated, with an average of 43,558,477 clean reads per library. The Q30 percentage in the 36 libraries averaged 91.93 % and GC percentage varied from 44.47 % to 47.74 %. These qualified reads were subsequently mapped to the *P. eburnea* reference genome, with over 82.7 % alignment rate across all libraries (Table S2). Heat mapping based on gene expression profiles revealed significantly different expression trends between sample groups (Fig. S2A). Principal component analysis (PCA) revealed that biological replicate samples from the same treatment group clustered together, demonstrating strong positive correlation within groups but weak correlation between different treatment groups (Fig. S2B–D), confirming the reliability of the sequencing data.

Gene expression analysis identified a total of 11,885 DEGs in leaves and 11,768 DEGs in roots in response to high calcium stress. The comparison group with the highest number of DEGs in leaves was 12 h vs.

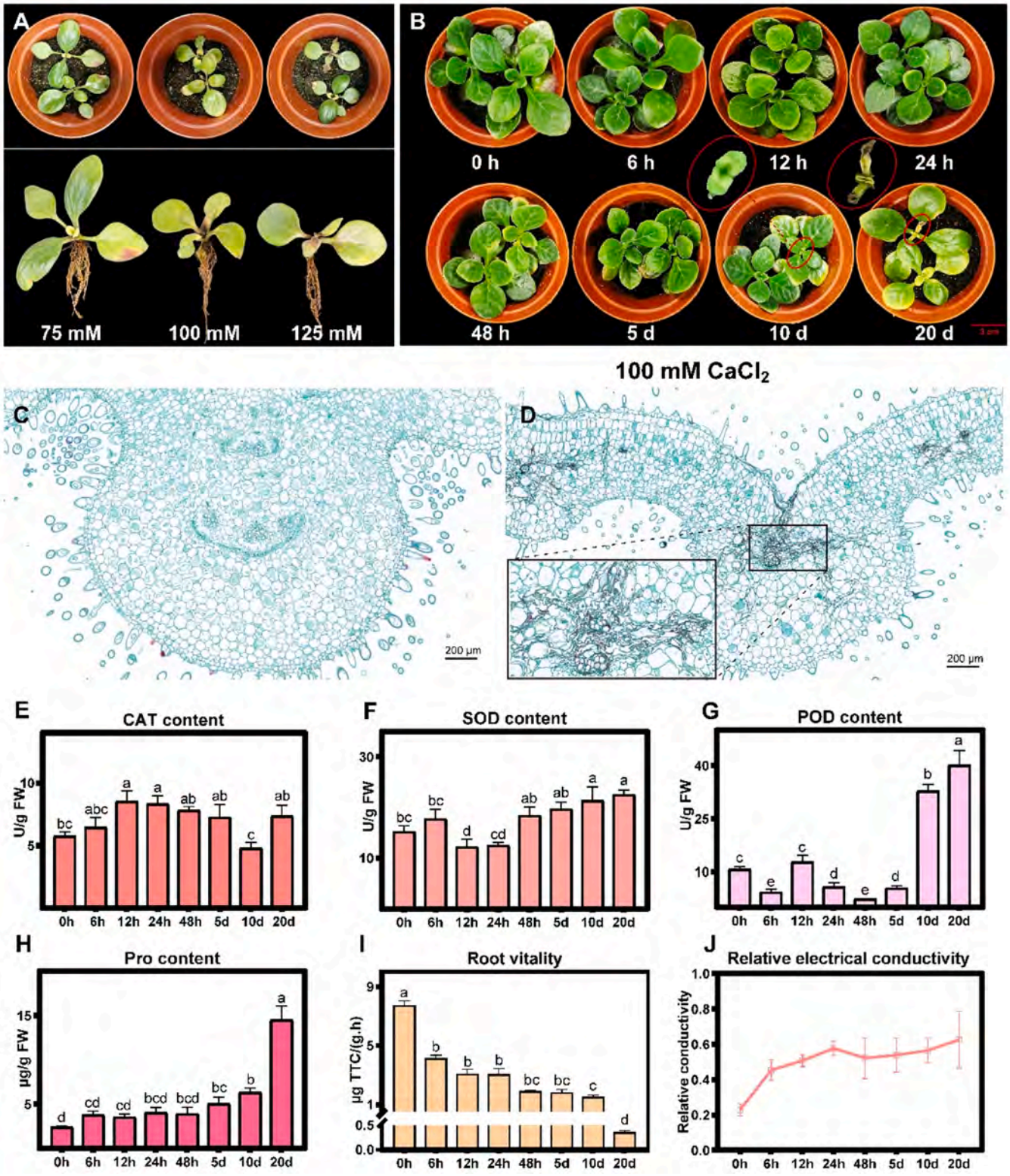

Fig. 1. Phenotype and physiological of *P. eburnea* under high calcium stress. (A) Phenotype under different concentrations of calcium stress. (B) Phenotype under 100 mM calcium stress at different time points. (C) Histological of normal leaves. (D) Histological of leaves after high calcium treatment. Physiological of leaves after high calcium treatment, (E) CAT content, (F) SOD content, (G) POD content, (H) Pro content, (I) Root vitality, (J) Relative electrical conductivity. Values are means ± SD of triplicate experiments.

0 h (7617), while in roots, it was 5 d vs. 0 h (Fig. 2 and Fig. S3). There were 734 and 1295 common DEGs among all comparison groups in leaves and roots, respectively. Interestingly, 6295 DEGs were found to response to calcium stress in both leaves and roots, including cation transporter proteins and TFs of the MYB family, bHLH family and WRKY family (Fig. 2A–C). This indicated the crucial roles of these genes in response to high calcium stress.

To validate the accuracy of the identified DEGs, we selected 12 genes

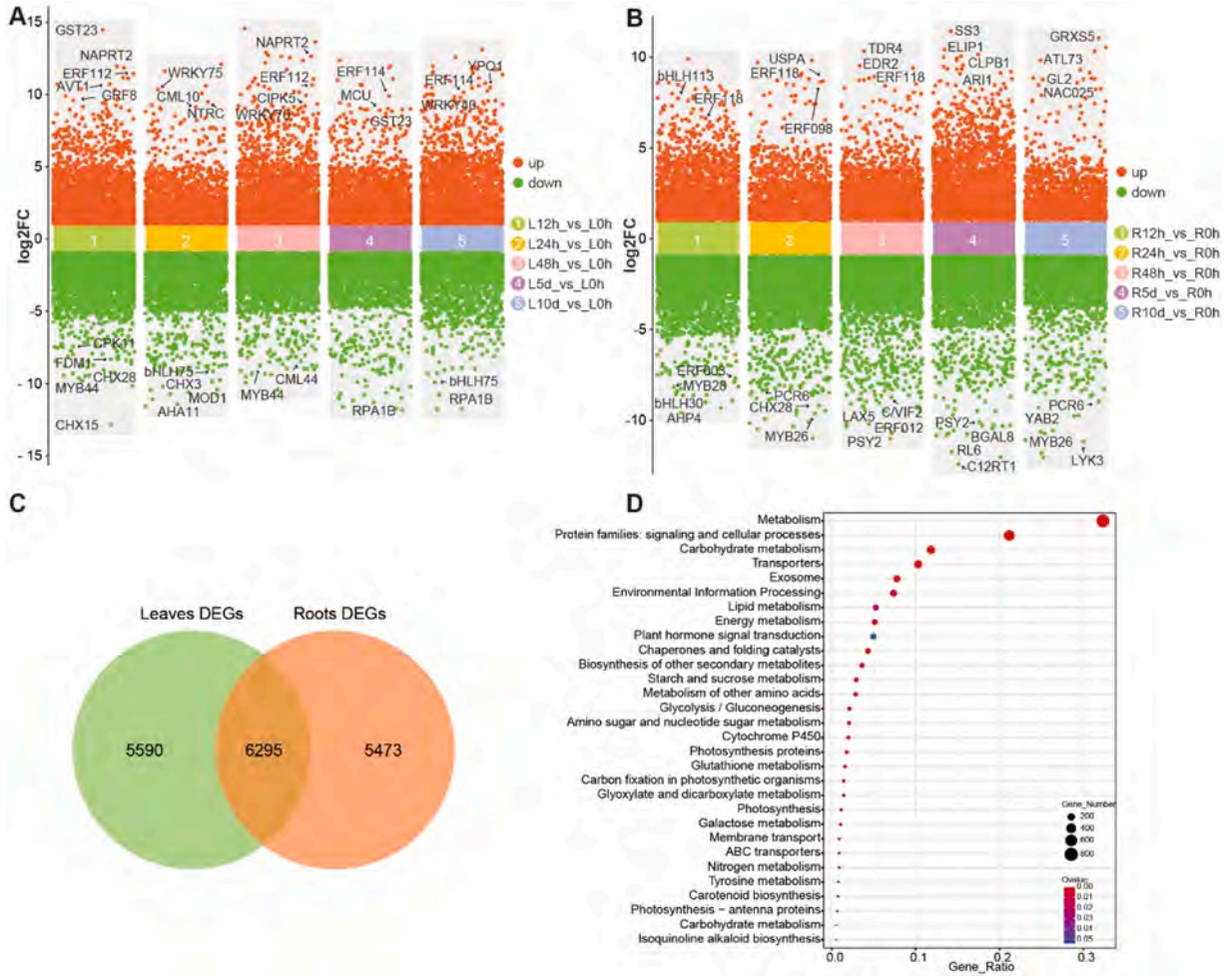

Fig. 2. Differentially expressed genes (DEGs) analysis in different periods of high calcium treatment. (A) DEGs in leaves. (B) DEGs in roots. (C) All common DEGs in the leaves and roots. (D) KEGG pathway enrichment of common DEGs in the leaves and roots.

for qRT-PCR validation and found the consistent expression trends with the RNA-seq results (Fig. S4). Furthermore, functional enrichment analysis of DEGs revealed distinct pathways involved in response to high calcium stress in leaves and roots. DEGs in the leaves were significantly involved in photosynthesis and oxidative stress pathways, with the GO terms enriched in structural constituent of ribosome, photosynthesis, photosystem, photosynthesis membrane, and oxidoreductase activity. In addition, these DEGs were assigned to KEGG pathways of ribosome, photosynthesis, carbon metabolism, pentose phosphate pathway, and flavonoid biosynthesis. For DEGs in the roots, they were enriched in GO terms of extracellular region, oxidoreductase activity, microtubule cytoskeleton, and plant-type cell wall organization (Fig. S3C and D; Fig. S5), and KEGG pathways of metabolic pathways, MAPK signaling pathway, plant-pathogen interaction, diterpenoid biosynthesis, and ABC transporters (Fig. S3E and F). As well, DEGs co-responding in leaves and roots were enriched in various pathways including metabolism, carbohydrate metabolism, transporters, plant hormone signal transduction, cytochrome P450, and membrane transporters (Fig. 2D).

3.3. *Time-ordered gene co-expression network in leaves under high calcium stress*

Genes with similar expression patterns tend to perform similar functions in the same pathway. To elucidate the temporal dynamics of gene expression in *P. eburnea* leaves under high calcium stress, we employed the Mfuzz software to cluster all transcripts into eight gene clusters (Fig. 3A). Following calcium treatment, gene expression of clusters 1, 2, and 3 decreased, while cluster 4 peaked after 12 hours of treatment. Clusters 5 and 6 increased and maintained relatively high levels after treatment, with clusters 7 and 8 peaking at 5 and 10 days, respectively.

To further dissect the regulatory network involved in the response to high calcium stress, we conducted the TO-GCN analysis with DEGs in leaves. Based on the expression trend of the seed gene, eight time series levels (Level 1–8) were assigned to DEGs, distinguishing 787 TFs and 10,490 non-TFs. Co-expression networks were constructed by assessing the correlation between the expression of TFs and non-TFs (Fig. 3B and Table S3). Interestingly, the gene expression peaks across eight time series levels corresponded precisely to the clustered expression pattern observed earlier, aligning with the time-course of calcium treatment (Fig. 3C). Genes in Level 1–3, which were downregulated by calcium treatment, were enriched in the photosynthesis pathway. The 12-hour treatment mark, considered the early stage of response to calcium stress, corresponded to Level 4 genes, which exhibited the largest network of regulatory relationships, and were enriched in calcium ion binding, transmembrane transport, and oxidoreductase activity pathways (Fig. 3B and D). Genes clustered in Level 5–8 were associated with metabolic processes, oxidoreductase activity, glycolytic process, and response to biotic stimulus, and were concerned with the middle and late stages of the response to calcium stress (Table S4). In particular, Level 8 was enriched in the membrane organization pathway.

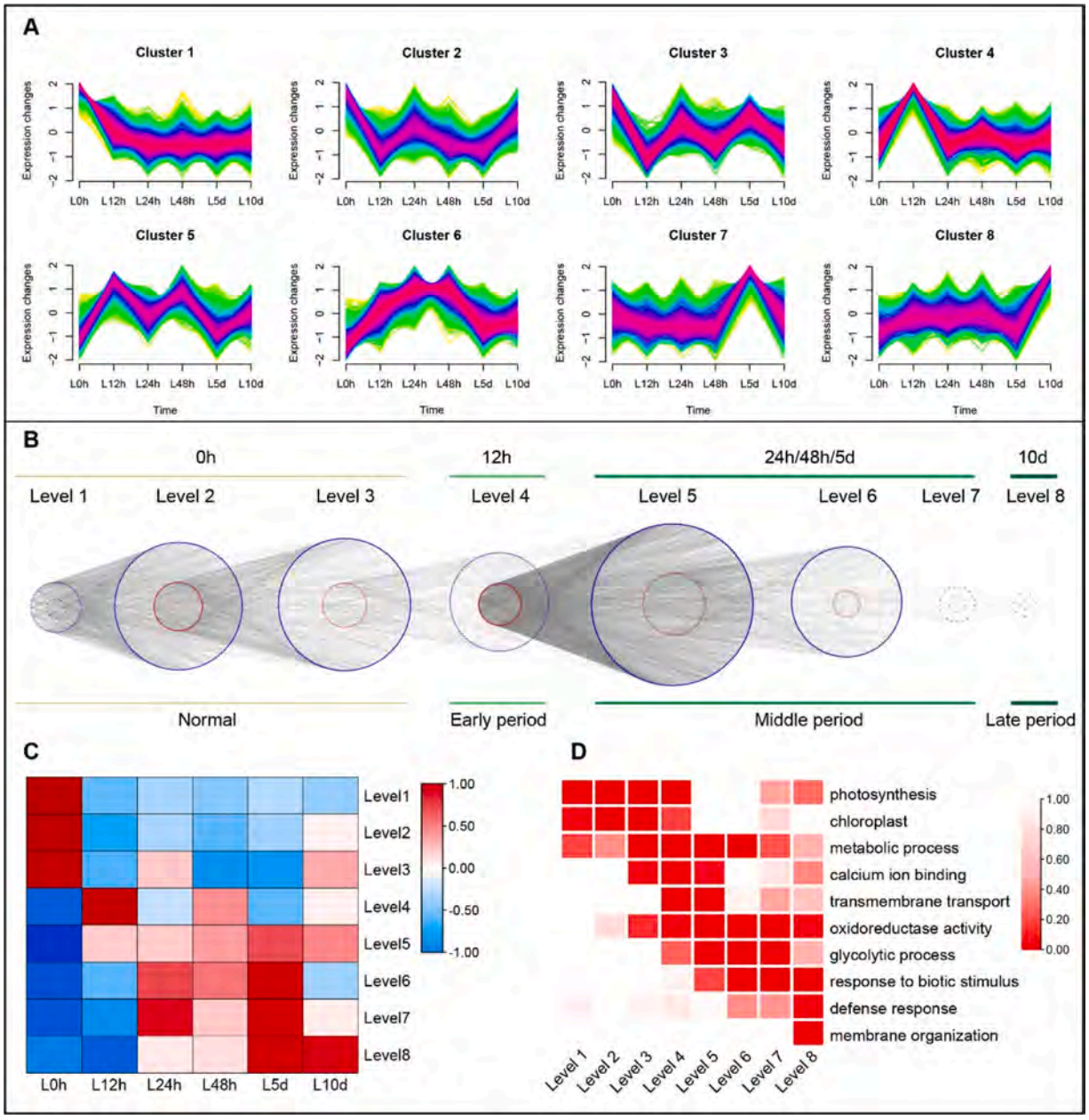

Fig. 3. Time-ordered gene co-expression network (TO-GCN) of the high calcium response in *P. eburnea*. (A) The expression pattern of all transcripts in leaves by Fuzzy c-means analysis method. (B) TO-GCN, and blue nodes on the outer layer represent non-Transcription-factor genes, red nodes represent Transcription factors. (C) Heatmap showing gene expression levels at different time points. (D) GO terms enrichment for co-expressed genes at each resolved Level. Darker colors represent lower *p*-values and more significant enrichment of GO terms.

3.4. Photosynthetic system responds to high calcium stress

Temporal expression analysis revealed significant enrichment of photosynthesis-related pathways in Level 1–4, including photosystem I (GO:0009522), photosystem II (GO:0009523), chloroplast (GO:0009507). The expression of these pathways decreased with prolonged treatment time, suggesting impaired regulation of photosynthetic system under high calcium stress. Subsequently, we identified photosynthesis-related genes and their potential TFs. A subnetwork was constructed containing 18 important genes involved in photosynthesis and 40 TFs (Fig. 4A). Photosystem II reaction center PSB28 protein (PSB28) acts as an assembled-cofactor to protect PSII from photodamage during assembly (Xiaol et al., 2021). In *P. eburnea*, the expression level of *PSB28* was dramatically suppressed by calcium treatment. Similarly, other genes including Chlorophyll a-b binding protein 7 (*CAB7*), Photosystem I reaction center subunit II (*psaD*), and Photosynthetic NDH subunit of lumenal location 3 (*PNSL3*) showed decreased expression levels in response to high calcium stress, as illustrated in the pie heatmap. There are 11 gene families that classify TFs involved in regulating photosynthesis. Among these TFs, the bHLH family was found to be the most abundant. It supported the discovery that bHLH involved in the regulation of chlorophyll metabolism processes (Moon et al., 2008). Overall, our findings suggest that high calcium stress disrupts the transcriptional regulation of photosynthesis, leading to the down-regulation of gene expression associated with photosynthesis.

3.5. Calcium signaling participates in hierarchical transcriptional network

The concentration of free calcium ions in the cytoplasm can trigger

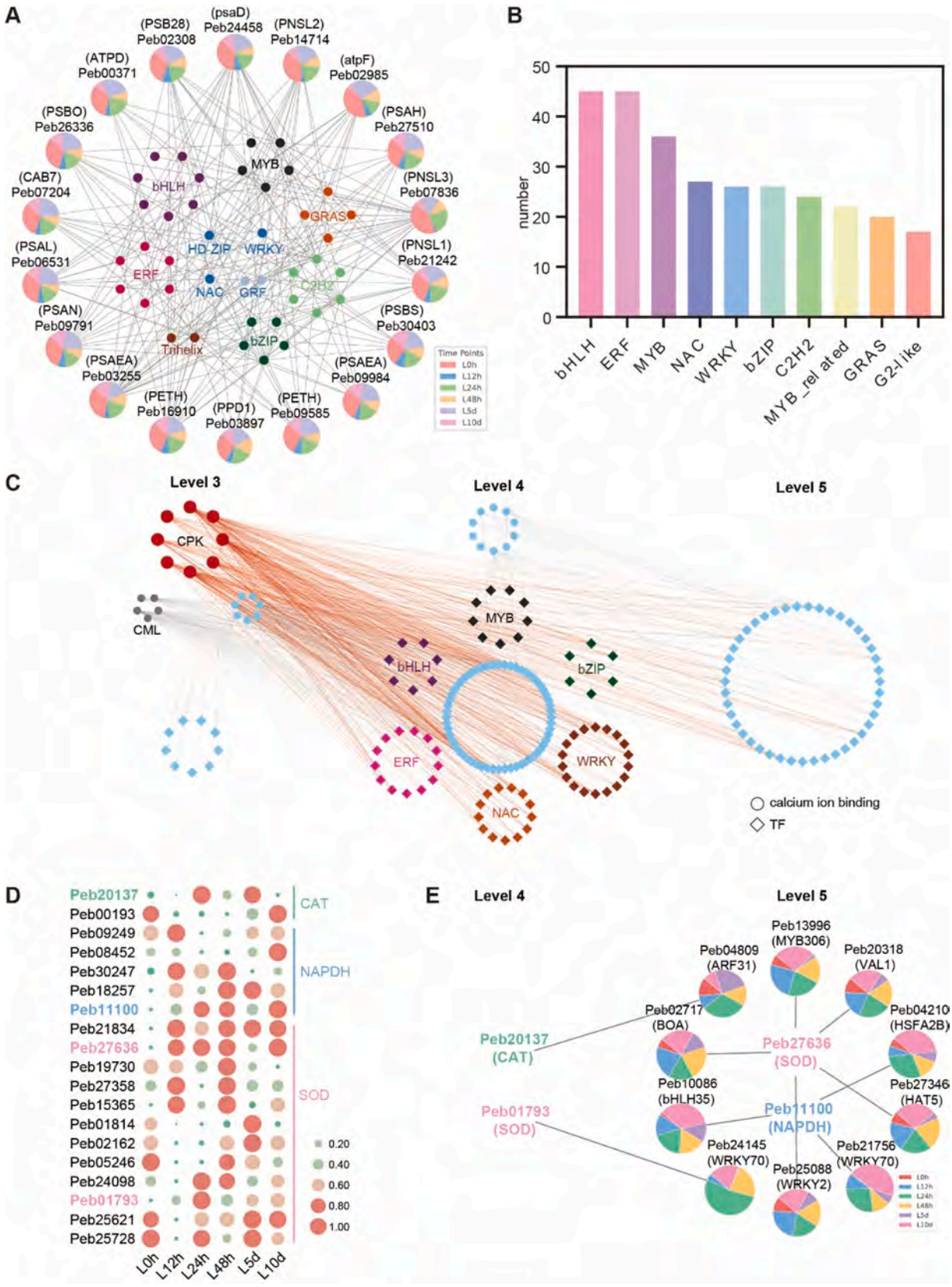

Fig. 4. Hierarchical regulatory networks of calcium stress-responsive genes in *P. eburnea*. (A) Subnetwork of photosynthesis-related protein and TFs. Pie charts illustrate the ratio of gene expression levels at different time points. TFs families on the inner layer were clustered by different colors. (B) Top 10 TFs families in the DEGs at 12 h compared to the control. (C) Subnetwork of calcium sensors and TFs. (D) Heatmap of oxidoreductase expression. The gene expression level is represented by the size and color of the circles. (E) Resolved hierarchical regulation for oxidoreductase gene.

signals that regulate various cellular activities. The TO-GCN analysis revealed that GO terms related to calcium ion binding were mainly enriched in the Level 3 and 4. Specifically, Ca^{2+} sensors, including Calcium-dependent protein kinases (CPKs), Calcium-binding proteins (CMLs) and Calcineurin B-like proteins (CBLs) were predominantly classified at Level 3. Furthermore, numerous TFs were co-expressed with the Ca^{2+} sensors and characterized at Level 4 (Fig. 4C). The most abundant TF families included WRKY, ERF, NAC, bHLH, MYB, and bZIP, consistent with the results observed in the DEGs of the 12 h and control comparator groups (Fig. 4B). The expression of these TFs peaked after 12 hours of treatment, indicating their involvement in regulating downstream target genes associated with the response to high calcium stress. Additionally, several other TFs were classified as Level 5. These findings collectively suggest that Ca^{2+} sensors play a vital role in the transcriptional response to high calcium stress, forming a hierarchical regulatory network by regulating the expression of TFs.

3.6. Calcium stress activates ROS pathway

Moderate concentrations of ROS play a regulatory role in plant stress responses, whereas excessive ROS can lead to oxidative stress (Mittler et al., 2022). In this study, the GO term of "oxidoreductase activity" was significantly enriched in Level 4–8 of the TO-GCN, suggesting that the ROS may act as a key signaling mediator in the response to calcium treatment in *P. eburnea*. Enzyme activity assays revealed activation of principal enzymes involved in the ROS elimination system, including POD, SOD and CAT, indicating the maintenance of ROS homeostasis (Fig. 1). Expressing analysis identified genes encoding these enzymes, particularly a class of POD enzymes known as NAPDHs (Fig. 4D), which were significantly up-regulated by calcium exposure. Combined with TO-GCN, the four significant genes and ten potential TFs were categorized into two Levels. *Peb20137 (CAT)* and *Peb01793 (SOD)* were regulated by *Peb04809 (ARF31)* and *Peb24145 (WRKY70)*, respectively, with peak expression observed after 24 h of calcium treatment. In Level 5, *Peb27636 (SOD)* and *Peb11100 (NAPDH)* exhibited sustained high expressed after calcium treatment and were regulated by eight TFs, including WRKY70 and WRKY2 (Fig. 4E). Given that WRKY TFs have been implicated in regulating NAPDH in response to stress (Adachi et al., 2015), our findings suggest that WRKY TFs may also play a crucial role in activating the ROS pathway in *P. eburnea* under high calcium stress.

3.7. Identification of key modules responding to high calcium stress

To deeper investigate the response mechanism to calcium treatment, we conducted the WGCNA on all transcripts to pinpoint key factors involved in responding to calcium stress. Thirteen co-expression modules were identified based on the similar expression patterns (Fig. 5A and B). Module-trait correlation analyses suggested that the lightsteelblue module was strongly correlated with leaf calcium content (Fig. 5B). This module contained 1869 genes functionally annotated with enriched GO terms such as calcium-dependent phospholipid binding, calmodulin binding, cation transport and metal ion transport

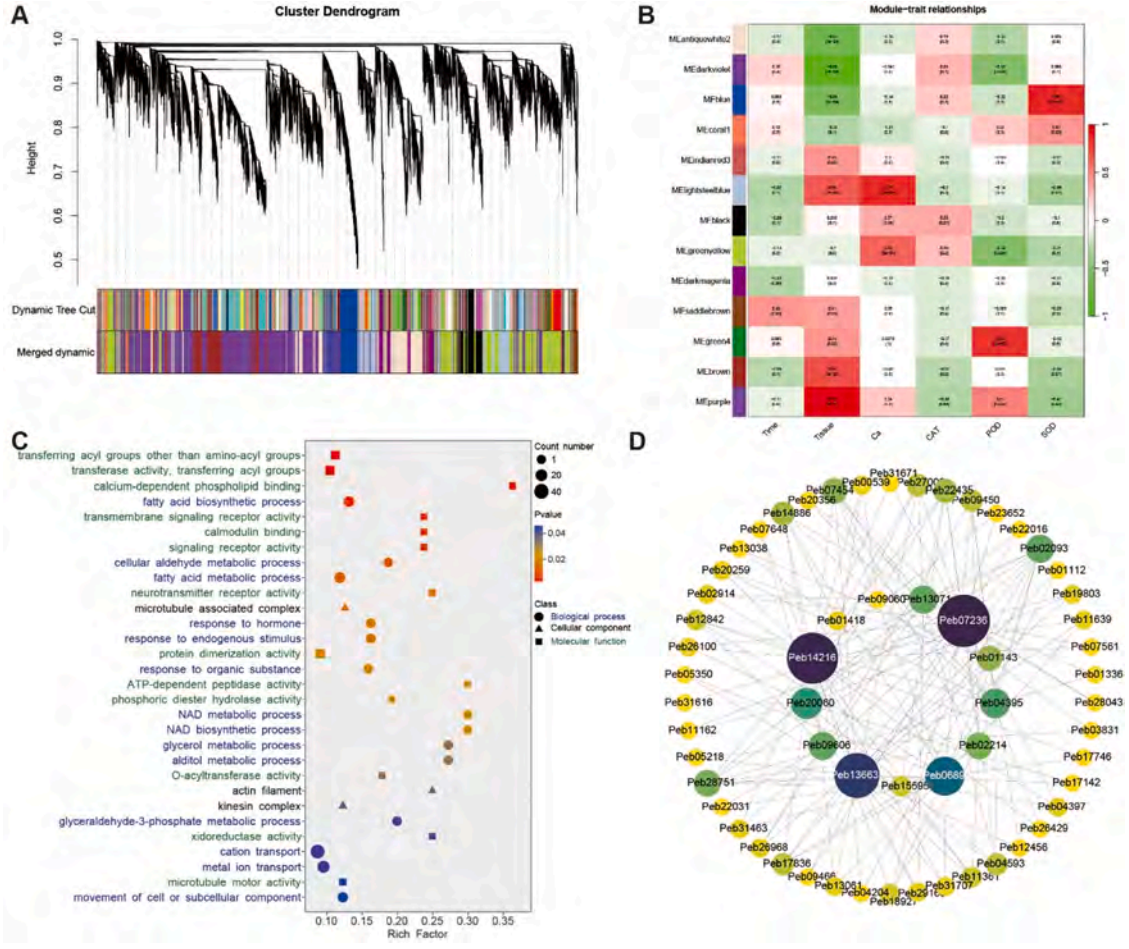

Fig. 5. Hub genes analysis of *P. eburnea* treated with high calcium stress. (A) Clustering dendrogram showing 13 modules of co-expressed genes identified in all samples. (B) Module-trait correlations under calcium treatment. Blue and red colors represent the negative and positive correlation, respectively. (C) GO enrichment analysis of the lightsteelblue module. (D) Regulatory network of calcium transporter and TFs in the lightsteelblue module. TFs on the outer layer and calcium transporter on the inner layer, the color and size of the circle represent the degree value.

(Fig. 5C), indicating its association with calcium ion transport. Within this module, thirteen candidate genes related to calcium ion transport were identified. A network was constructed to illustrate interactions between these genes and co-expressed TFs, highlighting the pivotal roles of two members of the CNGC family (Fig. 5D). The expression of *Peb13663 (PebCNGC2)* significantly exceeded that of *Peb20060 (PebCNGC4)* and exhibited a similar expression pattern, with both genes initially increasing in expression followed by a decrease after calcium treatment (Table S5). In *Arabidopsis*, *AtCNGC2* and *AtCNGC4*, which belong to the same *CNGC* subgroup, interact to form a heteromeric channel for their ion transport functions (Dietrich et al., 2020). This prompted us to speculate on potential functional redundancy between these two genes in *P. eburnea*, leading us to focus further analyses on *PebCNGC2*.

3.8. Identification of PebCNGC2-interacting TFs

To identify the subcellular localization of PebCNGC2, the PebCNGC2-GFP fusion protein was expressed in *N. benthamiana* leaves. The result showed that PebCNGC2 was co-localized not only with the plasma membrane marker AtCBL1, but was also in the nucleus (Fig. 6A). In conjunction with TO-GCN and WGCNA analyses, ten TFs highly correlated with *PebCNGC2* expression were identified within the light-steelblue module (Fig. 6B). Among these TFs, *Peb17836 (ANL2)* and *Peb07454 (ATML1)* exhibited the strongest correlation with *PebCNGC2*, with *Peb15384 (BZR1)* showing the highest expression. Besides, results from transcriptional binding site prediction (Table S6) suggested that all three TFs have the potential to bind to the *PebCNGC2* promoter (Fig. 6C). Subsequently, we employed the yeast one-hybrid system to investigate whether these three TFs could directly bind to the *PebCNGC2* promoter. In comparison to the negative control group, yeast strains that transformed with the *PebATML1-pGADT7* and *proPebCNGC2-pAbAi* vectors exhibited enhanced growth in the screening medium, as well as in the positive control. The evidence suggested that PebATML1 (Peb07454) directly binds to the *PebCNGC2* promoter, excluding PebANL2 (Peb17836) and PebBZR1 (Peb15384) (Fig. 6D). We further examined the expression of *PebATML1* and *PebCNGC2* by qRT-PCR, confirming a co-expression pattern between *PebATML1* and *PebCNGC2* (Fig. 6E). The dual-luciferase (LUC) reporter system was also employed to determine the regulatory relationship of *PebATML1* to *PebCNGC2*. A visible fluorescence signal was observed when co-expressing the *PebCNGC2pro::LUC* construct with the empty effector vector, with the signal markedly enhanced by co-expressing the PebATML1 protein (Fig. 6F–H). These findings strongly suggest that PebATML1 can bind directly to the *PebCNGC2* promoter, enhancing the expression of this gene during the pre-calcium treatment period.

4. Discussion

In karst regions, where calcium stress is a ubiquitous abiotic environmental stressor, plants are adversely affected at various levels, from physiological to molecular (Feng et al., 2022; Hepler, 2005). Although there have been many studies on Ca^{2+} signaling, the mechanisms underlying plant tolerance to high Ca^{2+} concentration remain largely unclear, especially at molecular level. In addition, physiological mechanisms of calcium tolerance or adaptation have been investigated in model plants or non-karst plants, such as *Arabidopsis* (Wang et al., 2017b), *Lemna minor* (Mazen et al., 2004), and *Lonicera confusa* (Wu et al., 2011). *Primulina* species, predominantly found in karst regions, exhibit strong calcium tolerance abilities (Qi et al., 2013) and has been used as a model for studying evolutionary adaptation to karst habitat environments (Feng et al., 2020; Gao et al., 2015; Ke et al., 2022). The time-series transcriptome under extreme condition is widely utilized for understanding the rapid response, medium-term adaptation, and long-term resistance to abiotic stress in plants (Chang et al., 2019; Xu et al., 2021; Zhao et al., 2023). In the present study, we employed *P. eburnea*, a plant broadly distributed in karst region, as a model to investigate the effects of exposure to lethal concentrations of calcium, and used TO-GCN to unravel the potential molecular regulatory network underlying the response to high calcium stress.

4.1. Physiological response to high calcium adaptation in P. eburnea

Calcium is not only an essential mineral for plants but also serves as a signaling molecule for plant cells to respond to changes in the external environment (Tian et al., 2020). However, high concentrations of Ca^{2+} can cause cytotoxicity, inhibiting plant growth and development. Our results showed that calcium treatment leads to leaf necrosis, particularly for cells near the leaf veins. Calcium ions are transported from the root system to the above-ground part via the xylem (White and Broadley, 2003), leading to higher calcium ion toxicity in cells near the leaf veins (Fig. 1A–D). After exposure to calcium, the high external calcium levels lowered the water potential outside the cells, leading to water shortage within the cells. To avoid losing too much water and keep the osmotic balance, plant cells produce substances like proline (Wani et al., 2018). In *P. eburnea* leaves, proline levels notably rose after calcium treatment (Fig. 1H). However, prolonged stress disrupted the cellular osmotic pressure homeostasis, leading to increased electrical conductivity and accumulation of ROS. The principal enzymes of the ROS elimination system swiftly responded to these alterations (Fig. 1E–G). It is noteworthy that exposure to calcium ion concentrations below 50 mM for one month does not adversely affect *P. eburnea*, whereas the same concentration is nearly lethal to wild-type *Arabidopsis* (Fig. 8B). This underscores the exceptional high calcium tolerance of *P. eburnea* as a karst plant. These physiological responses to high calcium stress have been observed in *P. eburnea*, highlighting the need to elucidate the molecular mechanisms underlying them.

4.2. Regulatory network of high calcium adaptation in P. eburnea

The regulatory network for plant adaptation to high calcium environments involves multiple biological processes, including adaptive physiological responses, calcium ion signaling, gene expression regulation, and calcium ion transport and accumulation. Transcription factors (TFs) are a core component of the complex regulatory network that orchestrates plant responses to high calcium conditions, capable of integrating multiple signaling pathways. To investigate the regulatory relationship between TFs and different response pathways in high calcium stress, we constructed TO-GCN based on a time-course transcriptomics analysis. We classified the differential genes in leaves into eight clusters, Level 1–8, corresponding to the different stages of response to calcium stress (Fig. 3). In the initial three Levels, there was a notable gene enrichment in the photosynthesis pathway, with the expression of these genes decreasing following calcium treatment (Fig. 4A). Calcium stress disrupts ionic balance, and thereby impeding the transportation of iron ions to protoporphyrin, which in turn reduces chlorophyll content and affects the photosynthesis (Ahire et al., 2014). For instance, *PSB28* regulates PSII activity, with *psb28* mutants exhibiting a light green phenotype (Jung et al., 2008). Additionally, photosystem I reaction center subunit XI (PSAL) can regulate photosynthesis by regulating the ratio of excitation energy partitioning between PSII and PSI (Hepworth et al., 2021). The chlorophyll a/b-binding (CAB) protein is verified to participate in thylakoid membrane assembly, thereby affecting photosynthesis (Green et al., 1991). We constructed regulatory network of genes and potential TFs predicts that bHLH, ERF, MYB, and WRKY are upstream regulators of these genes (Fig. 4A). The functions of these TFs in the regulation of photosynthesis have been partially elucidated in other plants. For instance, the LHC Regulating MYB (LRM) regulates the adaptation of the light harvest pigment-protein complexes (LHCs) to different light intensities in marine diatom (Agarwal et al., 2022). Do et al. (2020) reported three ERF TFs that positively regulate chloroplast division under salt stress in

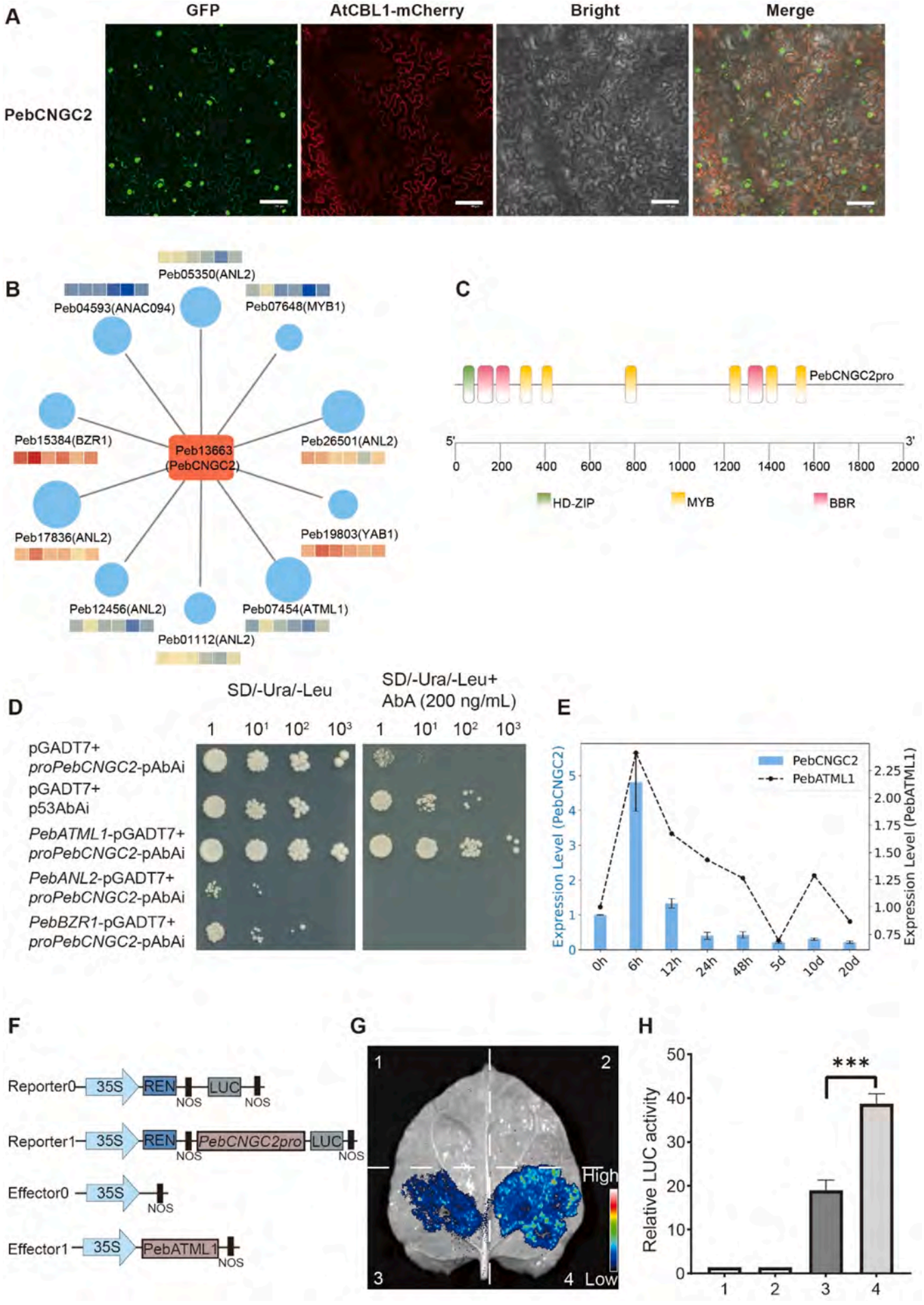

(caption on next page)

Fig. 6. PebATML1 binds to the promoter and enhances *PebCNGC2* expression under early calcium stress. (A) Subcellular localization of PebCNGC2 protein in *N. benthamiana* leaves. AtCBL1-mCherry was used as a plasma membrane location maker. Bars = 100 μm. (B) Relation network of PebCNGC2 and predicted TFs. Circles size represents the degree of correlation. TFs expression is visualized by a heat map, with levels of expression ranging from blue to red. (C) TFs binding sites in the promoter of *PebCNGC2*. (D) Yeast one-hybrid assay displaying the interaction between PebCNGC2 and TFs. p53AbAi acted as a positive control. (E) The expression levels of *PebCNGC2* and *PebATML1* under high calcium stress. (F) Constructed vectors used in dual-LUC assays. (G) Luciferase assay of PebCNGC2 and PebATML1 in *N. benthamiana* leaves. 1, Reporter0 + Effector0; 2, Reporter0 + Effector1; 3, Reporter1 + Effector0; 4, Reporter1 + Effector1. (H) Fluorescence intensity in dual-LUC assays. Values are means ± SD (n = 3; ***$P < 0.001$).

moss. Overexpression of *AhWRKY75* (a WRKY IIc subfamily member) enhanced photosynthesis and as a result improved salt stress tolerance in transgenic peanut lines (Zhu et al., 2021). These findings indicate that the photosynthesis process participates in the response of cationic stress (e.g. Na^+ and Ca^{2+}). In addition, WRKYs have been reported as potentially the most important TF family to ameliorate the drought or salt tolerance in *Primulina* species (Feng et al., 2020). However, the mechanisms of this amelioration require further investigation through additional works.

Ca^{2+} plays a crucial role in intracellular signal transduction in plants, activating responses to various stresses. This activation involves the decoding of calcium signals by an array of Ca^{2+} binding proteins, which are crucial for plants to effectively respond to stress. Different Ca^{2+} binding proteins exhibit varied responses to multiple abiotic stresses. For example, AtCDPK23 (a calcium-dependent protein kinase family member) negatively regulates response to drought and salt stress in Arabidopsis (Ma and Wu, 2007). Conversely, in cotton, GhCDPK60 enhances drought resistance through positive regulation (Yan et al., 2022). Calcineurin B-like proteins (CBLs) and CBL-interacting protein kinases (CIPKs) interact to decode calcium signals. When activated by calcium signals, CBL1/9 and CIPK1 can trigger a regulatory mechanism that phosphorylates the ABA receptor PYLs, resulting in negative regulation of drought stress (You et al., 2023). Furthermore, CBL2/3 and CIPK3/9/23/26 are involved in the transport of Mg^{2+} into vacuoles, crucial for maintaining normal plant growth in high Mg^{2+} environments (Tang et al., 2015). Calmodulin (CaM) and Calmodulin-like (CML) proteins are also calcium-binding proteins involved in the response to salt stress (Dong et al., 2022; Yuenyong et al., 2018). In our study, under high Ca^{2+} treatment, calcium signaling in *P. eburnea* was mainly decoded by CPK, CBL/CIPK and CML. In the developed calcium signaling regulatory sub-network (Fig. 4C), we categorized eight CPK genes and five CML genes as Level 3 components. Moreover, we identified several TFs interacting with them in Level 4, including WRKY, MYB, ERF, and bHLH. TFs play a crucial role in plant signaling pathways implicated in responses to abiotic stress. AtMYB2 responds to the salt-induced Ca^{2+} signaling pathway mediated by CaM, leading to proline accumulation and salt tolerance (Yoo et al., 2005). CML has been implicated in regulating heat shock transcription factors (HSFs) in response to heat stress (Raina et al., 2021). CaCDPK29 in pepper indirectly increases heat tolerance by promoting the expression of the *CaWRKY40* gene (Yang et al., 2022). Therefore, we hypothesize that the signals generated by Ca^{2+} influx under high calcium stress are decoded by CPKs and CMLs, which in turn induce these downstream TFs to respond to high calcium stress and confer plant tolerance.

Under stress, plants are able to scavenge reactive oxygen radicals and reduce their oxidative effects on cells through enzymes in the antioxidant enzyme system. In tobacco, NADPH oxidase, a pivotal enzyme in ascorbic acid biosynthesis pathway, is regulated by the MAPK-WRKY pathway (Adachi et al., 2015). Overexpressing of *GmNAC2* in tobacco reduces stress tolerance through negative regulation of *SOD* expression (Jin et al., 2013). Conversely, overexpression of *GmMYB84* in soybeans up-regulates SOD expression, resulting in improved drought tolerance in the transgenic lines (Wang et al., 2017a). A *bHLH* gene cloned from *Poncirus trifoliata* modulates ROS levels by regulating the *CAT* gene, thereby increasing cold tolerance in *Citrus grandis* (Geng et al., 2019). These studies indicate that TFs regulate oxidoreductases and are involved in the ROS elimination pathway. In our study, we also identified several essential enzyme coding genes for eliminating ROS increased their expression under high calcium condition (Figs. 1 and 4). ROS is not only a toxic molecule that inhibits cellular activities, it is also capable of acting as a signaling molecule that drives numerous signaling cascades (Ali et al., 2023). Under high calcium stress, multiple TFs involved in maintaining ROS homeostasis to enhance *P. eburnea* adaptation to calcium treatment. It is noteworthy that calcium sensors can integrate the calcium and ROS signaling in response to abiotic stress (Ali et al., 2023). The analysis of TO-GCN shows that calcium sensors, such as CML and CPK, are at Levels 3–5 associated with the ROS system and cross-regulate several families of TFs, indicating that they collectively play a regulatory role in the adaptation of the *P. eburnea* to high calcium treatment.

Plants primarily absorb and translocate calcium from the soil to leaf via the root system (White and Broadley, 2003). In environments with elevated calcium levels, the roots initially encounter high calcium ion concentrations. This raises the question of whether the root system's response to high calcium is similar to that of the leaves, elucidating the uniformity or divergence in their adaptation mechanisms. We also constructed a TO-GCN of differentially expressed genes in roots, which was divided into 8 Levels (Fig. 7). From Level 1 to Level 8, the quantity of TFs generally exhibits a decreasing trend, with a slight increase at Level 5. This indicates a rapid response of TFs during the early stages of high calcium treatment, mirroring the results observed in leaves (Fig. 7A). However, diverging from the expression pattern in leaves, the majority of genes in roots reach their expression peak between 12 and 48 hours after calcium treatment, markedly faster than in leaves (Fig. 7B). This accelerated response is intricately linked to the physiological role of roots in calcium translocation, underscoring a distinct temporal dynamic in gene expression between roots and leaves under high calcium conditions. Calcium treatment significantly enriched differentially expressed genes in root metabolic pathways, including Cytochrome P450, Starch and sucrose metabolism, and Glutathione metabolism. (Fig. 7C). Among these, Glutathione metabolism is particularly critical for plant resistance, engaging in key physiological processes essential for the detoxification of ROS and the maintenance of redox homeostasis (Ali et al., 2023). Consequently, it is evident that the root system exhibits a rapid response to high calcium stress, bolstering its resilience against unfavorable conditions through the activation of multiple metabolic pathways.

4.3. Molecular mechanism of high calcium adaptation in P. eburnea

After outlining the regulatory network of *P. eburnea* in response to high calcium stress, it remains unclear which genes are central to the resistance to the toxicity of high calcium. Weighted correlation network analysis (WGCNA) is an effective method for identifying highly synergistically altered gene modules and candidate gene targets based on the correlation between gene modules and traits, and has been used to screen hub genes under a variety of abiotic stresses (Langfelder and Horvath, 2008; Li et al., 2021; Mo et al., 2022; Sun et al., 2023; Wang et al., 2021). Using WGCNA, we identified 13 modules and determined that the lightsteelblue module is the core response module under high calcium stress (Fig. 5). This module is enriched with various calcium transporter proteins, including ACAs, CNGCs, CAXs and ANNs. ACA (Ca^{2+}-ATPase subfamily), considered efflux transporter, regulate calcium content, as evidenced by *GmACA7* in soybean seeds (Malle et al., 2020). The Ca^{2+}/cation antiporter (CaCA) transports Ca^{2+} from the cytoplasm to the vacuole for isolation and to prevent intracellular

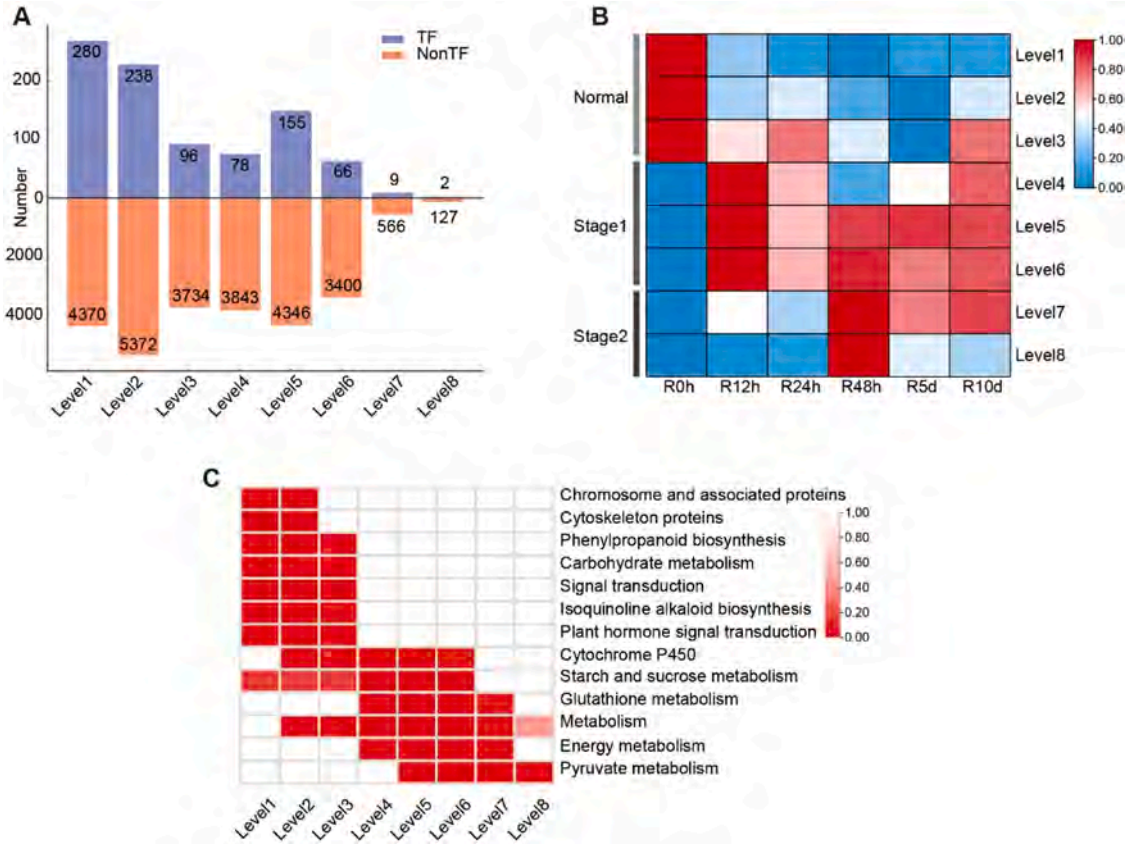

Fig. 7. TO-GCN of the high calcium response in Root. (A) The number of TFs and non-TFs in Level 1–8. (B) Heatmap showing gene expression levels at different time points. (C) KEGG enrichment for co-expressed genes at each resolved Level. Darker colors represent lower *p*-values and more significant enrichment of KEGG pathways.

accumulation of calcium ions (He et al., 2022). Cyclic nucleotide-gated ion channel (CNGC) mediates Ca^{2+} influx into the cytoplasm and is distributed in the plasma membrane, nucleus and other organelles (Charpentier et al., 2016; Christopher et al., 2007). CNGCs can participate in plant innate immunity not only through phosphorylation modifications but also by regulating calcium signaling in response to abiotic stress (Dietrich et al., 2020; Tian et al., 2019). In the present study, *PebCNGC2* was confirmed as a core gene in response to high calcium stress in *P. eburnea*, with homology to *AtCNGC2* in *Arabidopsis*. AtCNGC2 is an important Ca^{2+} channel at the plasma membrane that mediates Ca^{2+} influx into leaf cells (Wang et al., 2017b). We have developed transgenic *Arabidopsis* lines overexpressing the *PebCNGC2* gene (Fig. 8A). Under high calcium conditions, these transgenic lines demonstrate enhanced tolerance compared to the wild type, exhibiting significantly greater fresh weight of leaves (Fig. 8B and C). It has been reported that in plants, calcium exists not only in a H_2O-soluble form but also as calcium chelated by cell wall components and calcium chelated by acidic compounds such as oxalates (Matthew et al., 2011). These forms of calcium can be sequentially extracted using water, acetic acid (AA), and hydrochloric acid (HCl), respectively. Upon treatment with 50 mM calcium, the accumulation of H_2O-soluble calcium in the transgenic lines is significantly reduced, while the content of AA-soluble calcium increases (Fig. 8D). It was verified that when calcium ion supply is increased, leaf cells of the at*cngc2* mutant are unable to effectively unload excess free calcium ions. This leads to an excessive accumulation of calcium ions in the extracellular space, resulting in calcium toxicity (Wang et al., 2017b). In this study, the overexpression of the *PebCNGC2* line enhanced the calcium ion unloading capacity, reducing the content of free calcium ions and alleviating cellular calcium toxicity. Moreover, Ca^{2+} is crucial for the structure and function of Photosystem II (PSII). Within PSII, calcium ions are components of the oxygen-evolving complex, directly participating in the water-splitting process and the release of oxygen (Debus, 1992). Under high calcium treatment, the Fv/Fm value of the wild-type plants is only about 0.4, indicating severe photosynthetic damage. Compared to the wild type, the photosystem II of the transgenic lines suffers less damage (Fig. 8E and F). These results demonstrate that overexpressing *PebCNGC2* enhances the plant's ability to tolerate high calcium stress and maintain calcium ion homeostasis. It holds significant potential for the improvement of high-calcium vegetable varieties and environmental restoration in karst regions with high calcium levels.

Although some of the functions of *AtCNGC2* have been described, the TFs that regulate *AtCNGC2* expression have not been reported. Here, we identified candidate TFs that regulating *PebCNGC2* and verified that ATML1 can bind directly to the *PebCNGC2* promoter, increasing its expression during the pre-calcium treatment period (Fig. 6). In conditions of high calcium, a lot of Ca^{2+} moves through the xylem from roots to leaves. Then, ATML1 activates PebCNGC2, causing a surge in expression. This moves the excess Ca^{2+} from outside the cells to inside them. ATML1 acts as a critical regulator in plant epidermal formation and differentiation (Iida et al., 2023). The double mutant of *atml1 hdg3* displayed abnormal cotyledon development and epidermal differentiation. In addition, ATML1 is involved in the development of both epidermal trichomes and stomatal lineages (Liu et al., 2020; Nakamura et al., 2006). It has been demonstrated that trichomes on the leaf epidermal surface can store calcium, and excess calcium can be excreted through stomata (Wu et al., 2011). Interestingly, a large number of trichomes are also found on leaf surface of *P. eburnea*. Further experimental evidence is required to demonstrate the calcium storage in *P. eburnea* leaf trichomes and to elucidate the mechanism of

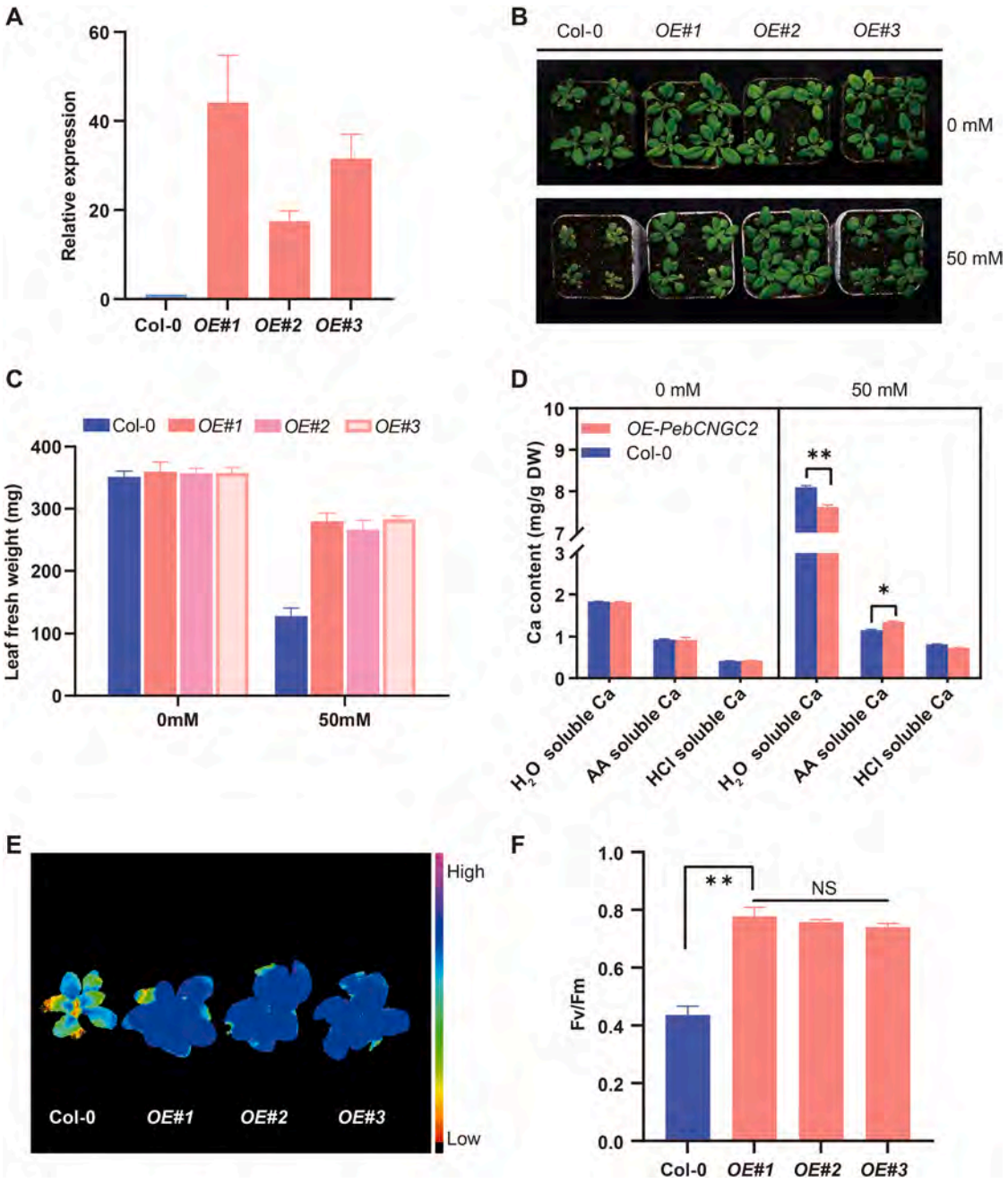

Fig. 8. Overexpressing *PebCNGC2* enhances the ability to withstand high calcium stress. (A) The expression level of the *PebCNGC2* overexpression transgenic lines. (B) The phenotypes of transgenic lines and Col-0 under treatment with 0 mM and 50 mM $CaCl_2$. (C) The leaf fresh weight and (D) Ca content of transgenic lines and Col-0 under treatment with 0 mM and 50 mM $CaCl_2$. (E), (F) The Fv/Fm value of transgenic lines and Col-0 under 50 mM $CaCl_2$ treatment. Values are means ± SD (*$P < 0.05$; **$P < 0.01$).

PebATML1-PebCNGC2 participation in the transportation and storage.

5. Conclusion

High calcium environments, characteristic of karst regions, significantly affect ecological and economic productivity. Studying the response to high-calcium soil-adapted species to high-calcium stress is crucial for understanding the broad molecular mechanisms of plant resistance to such environments. In this study, we conducted a comprehensive analysis of the physiological and transcriptomic effects of lethal concentrations of calcium stress on *P. eburnea* under time series conditions. Based on the TO-GCN and WGCNA, the regulatory networks, which include both TFs and non-TFs, are predicted to elucidate potential regulatory mechanisms for the response to high calcium stress. In conclusion, as Fig. 9 depicted, Ca^{2+} signals generated by the influx of Ca^{2+} into the cytoplasm are decoded by calcium sensors, which activate a diverse array of TFs responsible for maintaining the stability of the photosynthetic system, scavenging excess reactive oxygen species, limiting further influx of extracellular Ca^{2+} and transfer excess Ca^{2+} from the cytoplasm into the vacuole. This comprehensive analysis sheds light on the molecular mechanism underlying the plant responses to high calcium stress at the transcriptional level. Our study identified the core role of CNGC2 and its regulator ATML1 in mediating the response to high calcium stress. These findings lay the foundation for the cultivation of high calcium economic crops and effective ecological management practices in regions characterized by high calcium

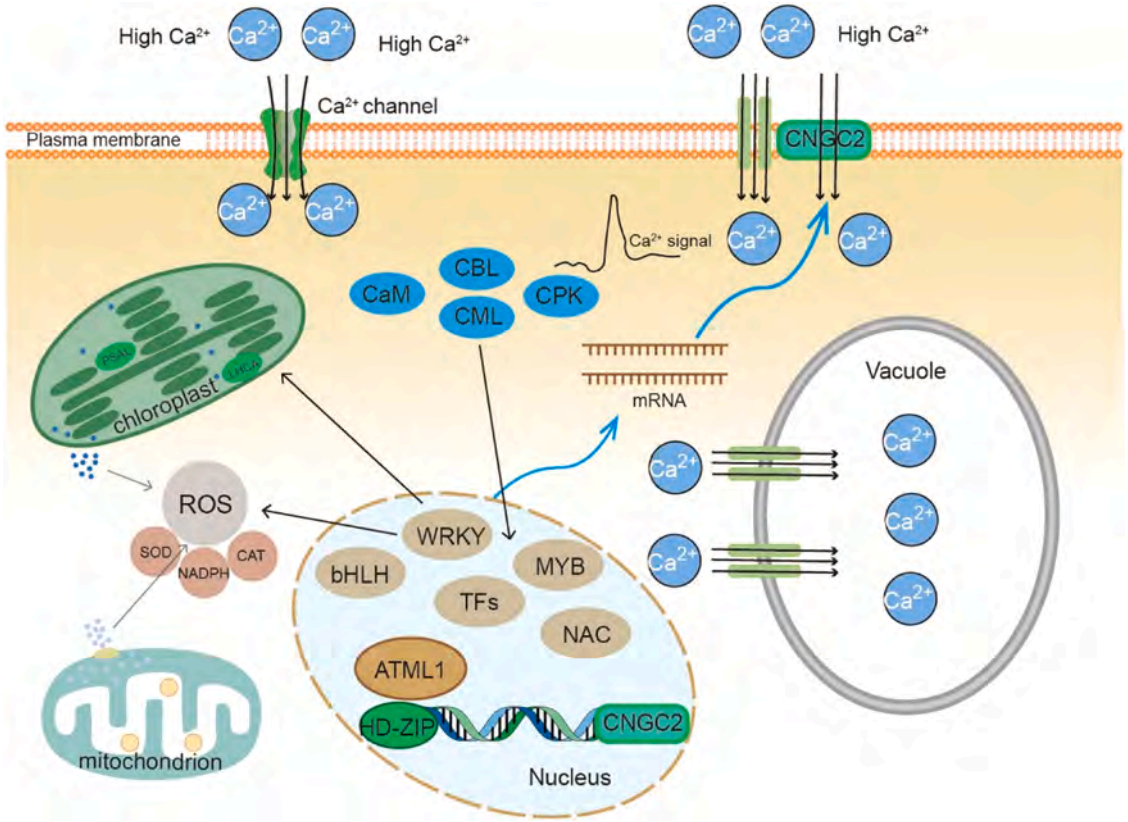

Fig. 9. Model of the molecular mechanism in response to high calcium stress in *P. eburnea*. Ca^{2+} sensors detect a significant increase in Ca^{2+} influx into the cytoplasm and activate downstream TFs in response to high calcium stress. They maintain the homeostasis of the photosynthetic system, activate SOD, CAT, and NADPH to remove reactive oxygen species and engage Ca^{2+} transporters in the tonoplast to capture Ca^{2+} in the vacuole. During the early stages of calcium stress, ATML1 enhances the expression of CNGC2 to transport Ca^{2+} to the leaf surface.

environments.

CRediT authorship contribution statement

Hongwen Huang: Writing – review & editing, Resources, Project administration, Investigation, Funding acquisition, Conceptualization. **Endian Yang:** Writing – original draft, Visualization, Validation, Data curation. **Qin Liu:** Methodology, Formal analysis, Data curation. **Yi Zhang:** Visualization, Formal analysis, Data curation. **Jie Zhang:** Validation, Resources, Methodology, Data curation. **Ziyi Lei:** Software, Methodology, Formal analysis, Data curation. **Chen Feng:** Writing – review & editing, Supervision, Project administration, Funding acquisition.

Declaration of Competing Interest

No potential conflict of interest was reported by the author(s).

Data Availability

Data will be made available on request.

Acknowledgments

This research was funded by the National Natural Science Foundation of China (32360060), the Biological Resources Program, Chinese Academy of Sciences (KFJ-BRP-007–013), and the Innovation Leading Talent Program in Jiangxi Province (JXSQ2023101107).

Appendix A. Supporting information

Supplementary data associated with this article can be found in the online version at doi:10.1016/j.indcrop.2024.119390.

References

Adachi, H., Nakano, T., Miyagawa, N., Ishihama, N., Yoshioka, M., Katou, Y., Yaeno, T., Shirasu, K., Yoshioka, H., 2015. WRKY Transcription factors phosphorylated by mapk regulate a plant immune nadph oxidase in *Nicotiana benthamiana*. Plant Cell 27 (9), 2645–2663. https://doi.org/10.1105/tpc.15.00213.

Agarwal, A., Di, R., Falkowski, P.G., 2022. Light-harvesting complex gene regulation by a MYB-family transcription factor in the marine diatom, *Phaeodactylum tricornutum*. Photosynth. Res. 153 (1-2), 59–70. https://doi.org/10.1007/s11120-022-00915-w.

Ahire, M.L., Laxmi, S., Walunj, P.R., Kishor, P.B.K., Nikam, T.D., 2014. Effect of potassium chloride and calcium chloride induced stress on in vitro cultures of *Bacopa monnieri* (L.) pennell and accumulation of medicinally important bacoside A. J. Plant Biochem. Biotechnol. 23 (4), 366–378. https://doi.org/10.1007/s13562-013-0220-z.

Ali, S., Tyagi, A., Bae, H., 2023. ROS interplay between plant growth and stress biology: challenges and future perspectives. Plant Physiol. Biochem. 203, 108032 https://doi.org/10.1016/j.plaphy.2023.108032.

Batistic, O., Waadt, R., Steinhorst, L., Held, K., Kudla, J., 2010. CBL-mediated targeting of CIPKs facilitates the decoding of calcium signals emanating from distinct cellular stores. Plant J. 61 (2), 211–222. https://doi.org/10.1111/j.1365-313X.2009.04045.x.

Borer, C.H., Hamby, M.N., Hutchinson, L.H., 2012. Plant tolerance of a high calcium environment via foliar partitioning and sequestration. J. Arid Environ. 85, 128–131. https://doi.org/10.1016/j.jaridenv.2012.06.004.

Bowler, C., Fluhr, R., 2000. The role of calcium and activated oxygens as signals for controlling cross-tolerance. Trends Plant Sci. 5 (6), 241–246. https://doi.org/10.1016/s1360-1385(00)01628-9.

Chang, Y.-M., Lin, H.-H., Liu, W.-Y., Yu, C.-P., Chen, H.-J., Wartini, P.P., Kao, Y.-Y., Wu, Y.-H., Lin, J.-J., Lu, M.-Y.J., Tu, S.-L., Wu, S.-H., Shiu, S.-H., Ku, M.S.B., Li, W.-H., 2019. Comparative transcriptomics method to infer gene coexpression networks and its applications to maize and rice leaf transcriptomes. Proc. Natl. Acad. Sci. USA 116 (8), 3091–3099. https://doi.org/10.1073/pnas.1817621116.

Charpentier, M., Sun, J., Martins, T.V., Radhakrishnan, G.V., Findlay, K., Soumpourou, E., Thouin, J., Very, A.-A., Sanders, D., Morris, R.J., Oldroyd, G.E.D., 2016. Nuclear-localized cyclic nucleotide-gated channels mediate symbiotic calcium oscillations. Science 352 (6289), 1102–1105. https://doi.org/10.1126/science.aae0109.

Cheng, N.H., Pittman, J.K., Shigaki, T., Lachmansingh, J., LeClere, S., Lahner, B., Salt, D. E., Hirschi, K.D., 2005. Functional association of *Arabidopsis* CAX1 and CAX3 is required for normal growth and ion homeostasis. Plant Physiol. 138 (4), 2048–2060. https://doi.org/10.1104/pp.105.061218.

Christopher, D.A., Borsics, T., Yuen, C.Y.L., Ullmer, W., Andeme-Ondzighi, C., Andres, M. A., Kang, B.-H., Staehelin, L.A., 2007. The cyclic nucleotide gated cation channel AtCNGC10 traffics from the ER via Golgi vesicles to the plasma membrane of *Arabidopsis* root and leaf cells. Bmc Plant Biol. 7, 48. https://doi.org/10.1186/1471-2229-7-48.

Debus, R.J., 1992. The manganese and calcium ions of photosynthetic oxygen evolution. Biochim. Et. Biophys. Acta (BBA)-Bioenerg. 1102 (3), 269–352. https://doi.org/10.1016/S0005-2728(05)80016-3.

Dietrich, P., Moeder, W., Yoshioka, K., 2020. Plant cyclic nucleotide-gated channels: new insights on their functions and regulation. Plant Physiol. 184 (1), 27–38. https://doi.org/10.1104/pp.20.00425.

Do, T.H., Pongthai, P., Ariyarathne, M., Teh, O.-K., Fujita, T., 2020. AP2/ERF transcription factors regulate salt-induced chloroplast division in the moss *Physcomitrella patens*. J. Plant Res. 133 (4), 537–548. https://doi.org/10.1007/s10265-020-01195-y.

Dong, Y., Liu, J., Li, P.-W., Li, C.-Q., Lu, T.-F., Yang, X., Wang, Y.-Z., 2018. Evolution of Darwin's *Peloric* Gloxinia (*Sinningia speciosa*) is caused by a null mutation in a pleiotropic TCP gene. Mol. Biol. Evol. 35 (8), 1901–1915. https://doi.org/10.1093/molbev/msy090.

Dong, Q., Wallrad, L., Almutairi, B.O., Kudla, J., 2022. Ca^{2+} signaling in plant responses to abiotic stresses. J. Integr. Plant Biol. 64 (2), 287–300. https://doi.org/10.1111/jipb.13228.

Feng, X., Peng, F., Yin, Z., Wang, J., Zhang, Y., Zhang, H., Fan, Y., Xu, N., Huang, H., Ni, K., Liu, X., Lei, Y., Jiang, T., Wang, J., Rui, C., Chen, C., Wang, S., Chen, X., Lu, X., Wang, D., Guo, L., Zhao, L., Li, Y., Wang, Y., Ye, W., 2022. Secondary metabolite pathway of SDG (secoisolariciresinol) was observed to trigger ROS scavenging system in response to Ca^{2+} stress in cotton. Genomics 114 (4), 110398. https://doi.org/10.1016/j.ygeno.2022.110398.

Feng, C., Wang, J., Wu, L., Kong, H., Yang, L., Feng, C., Wang, K., Rausher, M., Kang, M., 2020. The genome of a cave plant, *Primulina huaijiensis*, provides insights into adaptation to limestone karst habitats. N. Phytol. 227, 1249–1263. https://doi.org/10.1111/nph.16588.

Feng, C., Xu, M., Feng, C., von Wettberg, E.J.B., Kang, M., 2017. The complete chloroplast genome of *Primulina* and two novel strategies for development of high polymorphic loci for population genetic and phylogenetic studies. Bmc Evolut. Biol. 17, 224. https://doi.org/10.1186/s12862-017-1067-z.

Gao, Y., Ai, B., Kong, H., Kang, M., Huang, H., 2015. Geographical pattern of isolation and diversification in karst habitat islands: a case study in the *Primulina eburnea* complex. J. Biogeogr. 42 (11), 2131–2144. https://doi.org/10.1111/jbi.12576.

Geng, J., Wei, T., Wang, Y., Huang, X., Liu, J.-H., 2019. Overexpression of *PtrbHLH*, a basic helix-loop-helix transcription factor from *Poncirus trifoliata*, confers enhanced cold tolerance in pummelo (*Citrus grandis*) by modulation of H_2O_2 level via regulating a *CAT* gene. Tree Physiol. 39 (12), 2045–2054. https://doi.org/10.1093/treephys/tpz081.

Green, B.R., Pichersky, E., Kloppstech, K., 1991. CHLOROPHYLL-A/B-BINDING PROTEINS - AN EXTENDED FAMILY. Trends Biochem. Sci. 16 (5), 181–186. https://doi.org/10.1016/0968-0004(91)90072-4.

Guo, F., Jiang, G., Yuan, D., Polk, J.S., 2013. Evolution of major environmental geological problems in karst areas of Southwestern China. Environ. Earth Sci. 69 (7), 2427–2435. https://doi.org/10.1007/s12665-012-2070-8.

He, F., Shi, Y.-J., Li, J.-L., Lin, T.-T., Zhao, K.-J., Chen, L.-H., Mi, J.-X., Zhang, F., Zhong, Y., Lu, M.-M., Niu, M.-X., Feng, C.-H., Ding, S.-S., Peng, M.-Y., Huang, J.-L., Yang, H.-B., Wan, X.-Q., 2022. Genome-wide analysis and expression profiling of Cation/H^+ exchanger (CAX) family genes reveal likely functions in cadmium stress responses in poplar. Int. J. Biol. Macromol. 204, 76–88. https://doi.org/10.1016/j.ijbiomac.2022.01.202.

Hepler, P.K., 2005. Calcium: A central regulator of plant growth and development. Plant Cell 17 (8), 2142–2155. https://doi.org/10.1105/tpc.105.032508.

Hepworth, C., Wood, W.H.J., Emrich-Mills, T.Z., Proctor, M.S., Casson, S., Johnson, M.P., 2021. Dynamic thylakoid stacking and state transitions work synergistically to avoid acceptor-side limitation of photosystem I. Nat. Plants 7 (1). https://doi.org/10.1038/s41477-020-00828-3.

Iida, H., Maehoenen, A.P., Juergens, G., Takada, S., 2023. Epidermal injury-induced derepression of key regulator *ATML1* in newly exposed cells elicits epidermis regeneration. Nat. Commun. 14 (1), 1031. https://doi.org/10.1038/s41467-023-36731-6.

Jia, B., Li, Y., Sun, X., Sun, M., 2022. Structure, function, and applications of soybean calcium transporters. Int J. Mol. Sci. 23 (22) https://doi.org/10.3390/ijms232214220.

Jin, H., Huang, F., Cheng, H., Song, H., Yu, D., 2013. Overexpression of the *GmNAC2* Gene, an NAC transcription factor, reduces abiotic stress tolerance in tobacco. Plant Mol. Biol. Report. 31 (2), 435–442. https://doi.org/10.1007/s11105-012-0514-7.

Jung, K.-H., Lee, J., Dardick, C., Seo, Y.-S., Cao, P., Canlas, P., Phetsom, J., Xu, X., Ouyang, S., An, K., Cho, Y.-J., Lee, G.-C., Lee, Y., An, G., Ronald, P.C., 2008. Identification and functional analysis of light-responsive unique genes and gene family members in rice. Plos Genet. 4 (8), e1000164 https://doi.org/10.1371/journal.pgen.1000164.

Ke, F., Vasseur, L., Yi, H., Yang, L., Wei, X., Wang, B., Kang, M., 2022. Gene flow, linked selection, and divergent sorting of ancient polymorphism shape genomic divergence landscape in a group of edaphic specialists. Mol. Ecol. 31, 104–118. https://doi.org/10.1111/mec.16226.

Kim, D., Langmead, B., Salzberg, S.L., 2015. HISAT: a fast spliced aligner with low memory requirements, 357-U121 Nat. Methods 12 (4). https://doi.org/10.1038/nmeth.3317.

Langfelder, P., Horvath, S., 2008. WGCNA: an R package for weighted correlation network analysis. Bmc Bioinforma. 9, 559. https://doi.org/10.1186/1471-2105-9-559.

Li, Y., Zheng, X., Tian, Y., Ma, C., Yang, S., Wang, C., 2021. Comparative transcriptome analysis of NaCl and KCl stress response in malus hupehensis rehd. Provide insight into the regulation involved in Na+ and K+ homeostasis. Plant Physiol. Biochem. 164, 101–114. https://doi.org/10.1016/j.plaphy.2021.04.022.

Liu, Z.H., Groves, C., Yuan, D.X., Meiman, J., 2004. South China karst aquifer storm-scale hydrochemistry. Ground Water 42 (4), 491–499. https://doi.org/10.1111/j.1745-6584.2004.tb02617.x.

Liu, W., Jiang, L., Liu, B., Liu, R., Xiao, Z., 2023. Monitoring the evolution process of karst desertification and quantifying its drivers in the karst area of Southwest China. Environ. Sci. Pollut. Res. 30 (59), 123335–123350. https://doi.org/10.1007/s11356-023-30920-y.

Liu, Z., Zhou, Y., Guo, J., Li, J., Tian, Z., Zhu, Z., Wang, J., Wu, R., Zhang, B., Hu, Y., Sun, Y., Yan, S., Li, W., Li, T., Hu, Y., Guo, C., Rochaix, J.-D., Miao, Y., Sun, X., 2020. Global dynamic molecular profiling of stomatal lineage cell development by single-cell RNA sequencing. Mol. Plant 13 (8), 1178–1193. https://doi.org/10.1016/j.molp.2020.06.010.

Love, M.I., Huber, W., Anders, S., 2014. Moderated estimation of fold change and dispersion for RNA-seq data with DESeq2. Genome Biol. 15 (12), 550. https://doi.org/10.1186/s13059-014-0550-8.

Ma, S.-Y., Wu, W.-H., 2007. AtCPK23 functions in *Arabidopsis* responses to drought and salt stresses. Plant Mol. Biol. 65 (4), 511–518. https://doi.org/10.1007/s11103-007-9187-2.

Malle, S., Morrison, M., Belzile, F., 2020. Identification of loci controlling mineral element concentration in soybean seeds. Bmc Plant Biol. 20 (1), 419. https://doi.org/10.1186/s12870-020-02631-w.

Matthew, G., Maclin, D., Bradleigh, J.H., Bo, X., Simon, J.C., Brent, N.K., Roger, A.L., Stephen, D.T., 2011. Calcium delivery and storage in plant leaves: exploring the link with water flow. J. Exp. Bot. 62 (7), 2233–2250. https://doi.org/10.1093/jxb/err111.

Mazen, A.M.A., Zhang, D., Franceschi, V.R., 2004. Calcium oxalate formation in *Lemna minor*: physiological and ultrastructural aspects of high capacity calcium sequestration. N. Phytol. 161, 435–448. https://doi.org/10.1111/j.1469-8137.2004.00923.x.

McAinsh, M.R., Pittman, J.K., 2009. Shaping the calcium signature. N. Phytol. 181 (2), 275–294. https://doi.org/10.1111/j.1469-8137.2008.02682.x.

Mittler, R., Zandalinas, S.I., Fichman, Y., Van Breusegem, F., 2022. Reactive oxygen species signalling in plant stress responses. Nat. Rev. Mol. Cell Biol. 23 (10), 663–679. https://doi.org/10.1038/s41580-022-00499-2.

Mo, S., Biao, A., Wang, Z., Lin, S., Yang, T., Pan, L., Wang, Y., Zeng, S., 2022. Spatio transcriptome uncover novel insight into the Lycium ruthenicum seedling tolerant to salt stress. Ind. Crops Prod. 177, 114502 https://doi.org/10.1016/j.indcrop.2021.114502.

Moon, J., Zhu, L., Shen, H., Huq, E., 2008. PIF1 directly and indirectly regulates chlorophyll biosynthesis to optimize the greening process in *Arabidopsis*. Proc. Natl. Acad. Sci. USA 105 (27), 9433–9438. https://doi.org/10.1073/pnas.0803611105.

Nakamura, M., Katsumata, H., Abe, M., Yabe, N., Komeda, Y., Yamamoto, K.T., Takahashi, T., 2006. Characterization of the class IV homeodomain-leucine zipper gene family in *Arabidopsis*. Plant Physiol. 141 (4), 1363–1375. https://doi.org/10.1104/pp.106.077388.

Pertea, M., Pertea, G.M., Antonescu, C.M., Chang, T.-C., Mendell, J.T., Salzberg, S.L., 2015. StringTie enables improved reconstruction of a transcriptome from RNA-seq reads. Nat. Biotechnol. 33 (3), 290. https://doi.org/10.1038/nbt.3122.

Qi, Q., Hao, Z., Tao, J., Kang, M., 2013. Diversity of calcium speciation in leaves of *Primulina* species (Gesneriaceae). Biodivers. Sci. 21 (6), 715–722. https://doi.org/10.3724/SP.J.1003.2013.08152.

Raina, M., Kisku, A.V., Joon, S., Kumar, S., Kumar, D., 2021. Calmodulin and calmodulin-like Ca^{2+} binding proteins as molecular players of abiotic stress response in plants. Calcium Transp. Elem. Plants 231–248. https://doi.org/10.1016/B978-0-12-821792-4.00001-1.

Schneider, C.A., Rasband, W.S., Eliceiri, K.W., 2012. NIH Image to ImageJ: 25 years of image analysis. Nat. Methods 9 (7), 671–675. https://doi.org/10.1038/nmeth.2089.

Serain, A.F., Silverio, S.E.B., De Lourenco, C.C., Nunes, V.K., Correa, W.R., Stefanello, M. E.A., Salvador, M.J., 2021. Development of *Sinningia magnifica* (Otto & A. Dietr.) Wiehler (Gesneriaceae) tissue culture for in vitro production of quinones and bioactive molecules. Ind. Crops Prod. 159, 113046 https://doi.org/10.1016/j.indcrop.2020.113046.

Sun, Z., Li, J., Guo, D., Wang, T., Tian, Y., Ma, C., Liu, X., Wang, C., Zheng, X., 2023. Melatonin enhances KCl salinity tolerance by maintaining K^+ homeostasis in *Malus hupehensis*. Plant Biotechnol. J. https://doi.org/10.1111/pbi.14129.

Tang, R.-J., Zhao, F.-G., Garcia, V.J., Kleist, T.J., Yang, L., Zhang, H.-X., Luan, S., 2015. Tonoplast CBL-CIPK calcium signaling network regulates magnesium homeostasis in *Arabidopsis*. Proc. Natl. Acad. Sci. USA 112 (10), 3134–3139. https://doi.org/10.1073/pnas.1420944112.

Tian, W., Hou, C., Ren, Z., Wang, C., Zhao, F., Dahlbeck, D., Hu, S., Zhang, L., Niu, Q., Li, L., Staskawicz, B.J., Luan, S., 2019. A calmodulin-gated calcium channel links

pathogen patterns to plant immunity. Nature 572 (7767), 131. https://doi.org/10.1038/s41586-019-1413-y.
Tian, W., Wang, C., Gao, Q., Li, L., Luan, S., 2020. Calcium spikes, waves and oscillations in plant development and biotic interactions. Nat. Plants 6 (7), 750–759. https://doi.org/10.1038/s41477-020-0667-6.
Verdan, M.H., Alves Stefanello, M.E., 2012. Secondary metabolites and biological properties of gesneriaceae species. Chem. Biodivers. 9 (12), 2701–2731. https://doi.org/10.1002/cbdv.201100246.
Verret, F., Wheeler, G., Taylor, A.R., Farnham, G., Brownlee, C., 2010. Calcium channels in photosynthetic eukaryotes: implications for evolution of calcium-based signalling. N. Phytol. 187 (1), 23–43. https://doi.org/10.1111/j.1469-8137.2010.03271.x.
Wang, Y., Kang, Y., Ma, C., Miao, R., Wu, C., Long, Y., Ge, T., Wu, Z., Hou, X., Zhang, J., Qi, Z., 2017b. CNGC2 Is a Ca^{2+} influx channel that prevents accumulation of apoplastic Ca^{2+} in the leaf. Plant Physiol. 173 (2), 1342–1354. https://doi.org/10.1104/pp.16.01222.
Wang, R., Shu, P., Zhang, C., Zhang, J., Chen, Y., Zhang, Y., Du, K., Xie, Y., Li, M., Ma, T., Zhang, Y., Li, Z., Grierson, D., Pirrello, J., Chen, K., Bouzayen, M., Zhang, B., Liu, M., 2021. Integrative analyses of metabolome and genome-wide transcriptome reveal the regulatory network governing flavor formation in kiwifruit (*Actinidia chinensis*). N. Phytol. 233 (1), 373–389. https://doi.org/10.1111/nph.17618.
Wang, N., Zhang, W., Qin, M., Li, S., Qiao, M., Liu, Z., Xiang, F., 2017a. Drought Tolerance Conferred in Soybean (*Glycine max*. L) by GmMYB84, a Novel R2R3-MYB Transcription Factor. Plant Cell Physiol. 58 (10), 1764–1776. https://doi.org/10.1093/pcp/pcx111.
Wani, S.H., Tripathi, P., Zaid, A., Challa, G.S., Kumar, A., Kumar, V., Upadhyay, J., Joshi, R., Bhatt, M., 2018. Transcriptional regulation of osmotic stress tolerance in wheat (*Triticum aestivum* L.). Plant Mol. Biol. 97 (6), 469–487. https://doi.org/10.1007/s11103-018-0761-6.
White, P.J., Broadley, M.R., 2003. Calcium in plants. Ann. Bot. 92 (4), 487–511. https://doi.org/10.1093/aob/mcg164.
Wu, G., Jia, H., Huang, Y., Gan, L., Fu, C., Zhang, L., Yu, L., Li, M., 2014. Characterization and molecular interpretation of the photosynthetic traits of *Lonicera confusa* in karst environment. Plos One 9 (6), e100703. https://doi.org/10.1371/journal.pone.0100703.
Wu, G., Li, M., Zhong, F., Fu, C., Sun, J., Yu, L., 2011. *Lonicera confusa* has an anatomical mechanism to respond to calcium-rich environment. Plant Soil 338 (1-2), 343–353. https://doi.org/10.1007/s11104-010-0549-1.
Xiaol, Y., Huang, G., You, X., Zhu, Q., Wang, W., Kuang, T., Han, G., Sui, S.-F., Shen, J.-R., 2021. Structural insights into cyanobacterial photosystem II intermediates associated with Psb28 and Tsl0063. Nat. Plants 7 (8), 1132. https://doi.org/10.1038/s41477-021-00961-7.
Xu, J., Nie, S., Xu, C.-Q., Liu, H., Jia, K.-H., Zhou, S.-S., Zhao, W., Zhou, X.-Q., El-Kassaby, Y.A., Wang, X.-R., Porth, I., Mao, J.-F., 2021. UV-B-induced molecular mechanisms of stress physiology responses in the major northern Chinese conifer *Pinus tabuliformis* Carr. Tree Physiol. 41 (7), 1247–1263. https://doi.org/10.1093/treephys/tpaa180.
Yan, M., Yu, X., Zhou, G., Sun, D., Hu, Y., Huang, C., Zheng, Q., Sun, N., Wu, J., Fu, Z., Li, L., Feng, Z., Yu, S., 2022. GhCDPK60 positively regulates drought stress tolerance in both transgenic *Arabidopsis* and cotton by regulating proline content and ROS level. Front. Plant Sci. 13, 1072584 https://doi.org/10.3389/fpls.2022.1072584.
Yang, S., Cai, W., Shen, L., Cao, J., Liu, C., Hu, J., Guan, D., He, S., 2022. A CaCDPK29-CaWRKY27b module promotes CaWRKY40-mediated thermotolerance and immunity to *Ralstonia solanacearum* in pepper. N. Phytol. 233 (4), 1843–1863. https://doi.org/10.1111/nph.17891.
Yang, L.-Y., Yi, P., Chen, J.-L., Li, Y.-H., Qiu, J.-L., Wang, Z.-Y., Fu, M., Yuan, C.-M., Huang, L.-J., Hao, X.-J., Gu, W., 2023. Chemical constituents of primulina eburnea (gesneriaceae) and their cytotoxic activities. Chem. Biodivers. https://doi.org/10.1002/cbdv.202300248.
Yang, E., Zheng, M., Zou, X., Huang, X., Yang, H., Chen, X., Zhang, J., 2021. Global transcriptomic analysis reveals differentially expressed genes involved in embryogenic callus induction in drumstick (*Moringa oleifera* Lam.). Int. J. Mol. Sci. 22 (22), 12130. https://doi.org/10.3390/ijms222212130.
Yi, H., Wang, J., Wang, J., Rausher, M., Kang, M., 2022. Genomic insights into inter- and intraspecific mating system shifts in *Primulina*. Mol. Ecol. 31 (22), 5699–5713. https://doi.org/10.1111/mec.16706.
Yoo, J.H., Park, C.Y., Kim, J.C., Heo, W.D., Cheong, M.S., Park, H.C., Kim, M.C., Moon, B. C., Choi, M.S., Kang, Y.H., Lee, J.H., Kim, H.S., Lee, S.M., Yoon, H.W., Lim, C.O., Yun, D.J., Lee, S.Y., Chung, W.S., Cho, M.J., 2005. Direct interaction of a divergent CaM isoform and the transcription factor, MYB2, enhances salt tolerance in *Arabidopsis*. J. Biol. Chem. 280 (5), 3697–3706. https://doi.org/10.1074/jbc.M408237200.
You, Z., Guo, S., Li, Q., Fang, Y., Huang, P., Ju, C., Wang, C., 2023. The CBL1/9-CIPK1 calcium sensor negatively regulates drought stress by phosphorylating the PYLs ABA receptor. Nat. Commun. 14 (1) https://doi.org/10.1038/s41467-023-41657-0.
Yuenyong, W., Chinpongpanich, A., Comai, L., Chadchawan, S., Buaboocha, T., 2018. Downstream components of the calmodulin signaling pathway in the rice salt stress response revealed by transcriptome profiling and target identification. Bmc Plant Biol. 18, 335. https://doi.org/10.1186/s12870-018-1538-4.
Zhang, B., Horvath, S., 2005. A general framework for weighted gene co-expression network analysis. Stat. Appl. Genet. Mol. Biol. 4, 17. https://doi.org/10.2202/1544-6115.1128.
Zhang, J., Zhang, Y., Feng, C., 2024. Genome-wide analysis of MYB Genes in *Primulina eburnea* (Hance) and identification of members in response to drought stress. Int. J. Mol. Sci. 25 (1), 465. https://doi.org/10.3390/ijms25010465.
Zhao, Y., Jia, K., Tian, Y., Han, K., El-Kassaby, Y.A., Yang, H., Si, H., Sun, Y., Li, Y., 2023. Time-course transcriptomics analysis reveals key responses of populus to salt stress. Ind. Crops Prod. 194, 116278 https://doi.org/10.1016/j.indcrop.2023.116278.
Zhu, H., Jiang, Y., Guo, Y., Huang, J., Zhou, M., Tang, Y., Sui, J., Wang, J., Qiao, L., 2021. A novel salt inducible WRKY transcription factor gene, *AhWRKY75*, confers salt tolerance in transgenic peanut. Plant Physiol. Biochem. 160, 175–183. https://doi.org/10.1016/j.plaphy.2021.01.014.